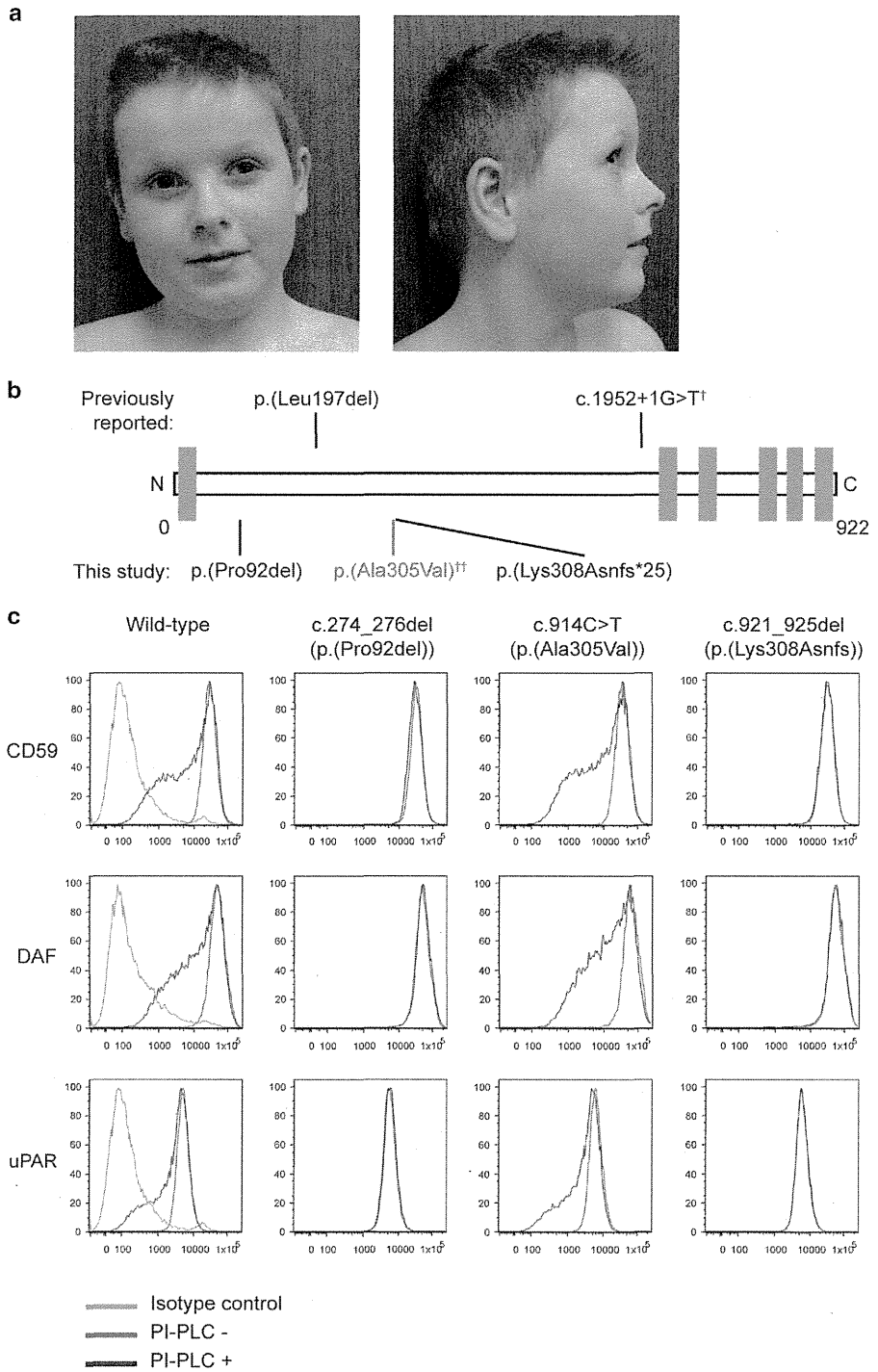

Figure 1 Phenotype of the affected individual and the functional analysis of the variants. (**a**) Photographs of the affected individual, note the upward slanting palpebral fissures, deep-set eyes, large ear lobes and prominent helices and antihelices. (**b**) Schematic representation of PGAP1-containing transmembrane domains (in green). The positions of the variants identified in this study and in the previous reports are indicated. †For this variant the effect on amino acid sequence was not studied. ††Considered as a variant without functional impact. (**c**) CHO cells deficient for *PGAP1* were used to investigate the expected structural abnormalities of the GPI anchors by testing the sensitivity of GPI-APs to PI-PLC. Wild-type *PGAP1* and the construct containing the variant c.914C>T (p.(Ala305Val)) rescued the sensitivity for PI-PLC strongly suggesting that this variant is benign. The *PGAP1* constructs containing the c.274_276del (p.(Pro92del)) and c.921_925del (p.(Lys308Asnfs*25)) variants did not increase the sensitivity for PI-PLC, suggesting that both are causal.

Table 1 Phenotype of individuals with *PGAP1* variants

	This study	*Murakami III-2*	*Murakami III-3*	*Novarino 1241-IV-3*	*Novarino 1241-IV-4*
Variant identified (Hg 19)	c.274_276del (p.(Pro92del)) and c.921_925del (p.(Lys308Asnfs*25))	c.589_591del (p.(Leu197del)) and c.589_591del (p.(Leu197del))	c.589_591del (p.(Leu197del)) and c.589_591del (p.(Leu197del))	c.1952+1G>T and c.1952+1G>T	c.1952+1G>T and c.1952+1G>T
Gender	M	F	M	M	M
Birth weight	3550 g (70th centile)	Normal	Normal	NA	NA
Gestational age (weeks)	38	Normal	Normal	NA	NA
Age at investigations (years$^{+months}$)	7^{+10}	4^{+5}	2^{+9}	6^{+6}	0^{+9}
Height	131 cm (50th centile)	96 cm (25th centile)	Normal	NA	NA
OFC	52.5 cm (50th centile)	46 cm (<5th centile)	47 cm (<5th centile)	NA	NA
Delayed development	+	+	+	+	+
Walking independently (years$^{+months}$)	2^{+6}	4^{+5}	–	–	–
First words (years$^{+months}$)	2^{+6}	–	–	NA	NA
Hypotonia	+	+	+	NA	NA
Brain imaging (MRI/CT)	Normal (MRI)	Pronounced brain atrophy (CT)	NP	Prominent cortical sulci and widened sylvian fissures (MRI)	Corpus callosum agnesis, vermis hypoplasia, defective myelination (MRI)
Hearing investigation	Normal	NP	NP	NA	NA
Ophthalmological examination	CVI, strabismus, nystagmus	NP	NP	–	–
Other abnormalities	Factor XII deficiency	Stereotypic movements, seizures	Stereotypic movements	Spasticity	Spasticity, distented abdomen
Dysmorphism	Upward slanting palpebral fissures, deep-set eyes, large ear lobes, prominent helices and antihelices, teeth showed extra mamelons with diminished enamel	Large ears, flattenend nasal bridge	Large ears, flattenend nasal bridge	NA	NA

Abbreviations: NA, not available; NP, not performend.

One marker of CDG syndromes can be the abnormal glycosylation of transferrin.[37] However, in the subclass of GPI anchor glycosylation defects, no abnormal transferrin is detectable, making this marker unreliable in diagnosing GPI anchor glycosylation defects, such as those caused by variants in *PGAP1*.

One other feature of CDG syndromes is the deficiency of coagulation factors.[37] However, factor XII deficiency has not been reported so far, neither has a direct functional link between factor XII and GPI-APs been made. Factor XII deficiency can be caused by variants in *F12*; a heterozygous variant can lead to an intermediated level of factor XII activity, whereas homozygous or compound heterozygous variants lead to almost no activity (<1%).[38,39] The current individual had a factor XII activity <1%, and a paternal inherited loss of function variant in *F12*, c.827G>A (p.(Trp276*)), but his father had a normal factor XII activity. The mother had an intermediate factor XII activity, but no variant could be identified in her exome results. Whether the variants in *PGAP1* are related to the factor XII deficiency is yet unclear.

Two other GPI anchor-modeling proteins, PGAP2 and PGAP3, are implicated in hyperphosphatasia with mental retardation syndrome, also named Mabry syndrome.[22–24] These individuals showed, in addition to ID, seizures, typical facial dysmorphisms and an increased alkaline phosphatase (ALP). This increase is due to diminished GPI-APs on the cell surface, resulting in less binding of ALP to the cell membrane and more ALP in the plasma.[22–24,40,41] ALP was not measured in the *PGAP1*-affected individuals, but in PGAP1-deficient cells, no diminished cell-surface expression of GPI-APs was measured, making elevated ALP levels less likely.[15] In addition, the typical facial dysmorphisms of Mabry syndrome, consisting of apparent hypertelorism, long palpebral fissures, short nose with broad nasal bridge and tip and tented upper lip vermillion, were not present in the here presented individual.

In conclusion, we identified novel *PGAP1* variants in an intellectual disabled boy with a proven functional loss of PGAP1 and showed for the first time the genetic association with cerebral visual impairment. Additional affected individuals will be required to gain better insights into pathophysiology and acquire knowledge of the clinical spectrum of this novel disorder.

CONFLICT OF INTEREST

The authors declare no conflict of interest.

ACKNOWLEDGEMENTS

We are grateful to the individual involved and his family for their support and cooperation. We thank the technical ophthalmological assistant P. Rison for his assistance during the ophthalmological examination. This work has been supported by grants from Stichting ODAS (to FNB and FPMC), Vereniging Bartiméus-Sonneheerdt (5781251 to FNB and FPMC), and the Dutch Organization for Health Research and Development (917-86-319 and 912-12-109 to BBAdV). In addition, this study was accomplished in part through the Center for Mendelian Genomics research effort funded by the National

Institutes of Health and supported by the National Human Genome Research Institute grant U54HG006542 to the Baylor-Hopkins Center for Mendelian Genomics.

1 Boonstra N, Limburg H, Tijmes N, van Genderen M, Schuil J, van Nispen R: Changes in causes of low vision between 1988 and 2009 in a Dutch population of children. *Acta Ophthalmol* 2012; **90**: 277–286.
2 Rahi JS, Cable N: Severe visual impairment and blindness in children in the UK. *Lancet* 2003; **362**: 1359–1365.
3 Dutton GN, Jacobson LK: Cerebral visual impairment in children. *Semin Neonatol* 2001; **6**: 477–485.
4 Bosch DG, Boonstra FN, Willemsen MA, Cremers FP, de Vries BB: Low vision due to cerebral visual impairment: differentiating between acquired and genetic causes. *BMC Ophthalmol* 2014; **14**: 59.
5 Bosch DG, Boonstra FN, Reijnders MR, Pfundt R, Cremers FP, de Vries BB: Chromosomal aberrations in cerebral visual impairment. *Eur J Paediatr Neurol* 2014; **18**: 677–684.
6 Bosch DG, Boonstra FN, Gonzaga-Jauregui C *et al*.: *NR2F1* mutations cause optic atrophy with intellectual disability. *Am J Hum Genet* 2014; **94**: 303–309.
7 Jensen H, Kjaergaard S, Klie F, Moller HU: Ophthalmic manifestations of congenital disorder of glycosylation type 1a. *Ophthalmic Genet* 2003; **24**: 81–88.
8 Morava E, Wevers RA, Cantagrel V *et al*.: A novel cerebello-ocular syndrome with abnormal glycosylation due to abnormalities in dolichol metabolism. *Brain* 2010; **133**: 3210–3220.
9 Enns GM, Shashi V, Bainbridge M *et al*.: Mutations in NGLY1 cause an inherited disorder of the endoplasmic reticulum-associated degradation pathway. *Genet Med* 2014; **16**: 751–758.
10 Jaeken J: Congenital disorders of glycosylation (CDG): it's (nearly) all in it! *J Inherit Metab Dis* 2011; **34**: 853–858.
11 Fujita M, Kinoshita T: GPI-anchor remodeling: potential functions of GPI-anchors in intracellular trafficking and membrane dynamics. *Biochim Biophys Acta* 2012; **1821**: 1050–1058.
12 Tiede A, Bastisch I, Schubert J, Orlean P, Schmidt RE: Biosynthesis of glycosylphosphatidylinositols in mammals and unicellular microbes. *Biol Chem* 1999; **380**: 503–523.
13 McConville MJ, Menon AK: Recent developments in the cell biology and biochemistry of glycosylphosphatidylinositol lipids (review). *Mol Membr Biol* 2000; **17**: 1–16.
14 Tanaka S, Maeda Y, Tashima Y, Kinoshita T: Inositol deacylation of glycosylphosphatidylinositol-anchored proteins is mediated by mammalian PGAP1 and yeast Bst1p. *J Biol Chem* 2004; **279**: 14256–14263.
15 Murakami Y, Tawamie H, Maeda Y *et al*: Null mutation in PGAP1 impairing Gpi-anchor maturation in patients with intellectual disability and encephalopathy. *PLoS Genet* 2014; **10**: e1004320.
16 Johnston JJ, Gropman AL, Sapp JC *et al*: The phenotype of a germline mutation in PIGA: the gene somatically mutated in paroxysmal nocturnal hemoglobinuria. *Am J Hum Genet* 2012; **90**: 295–300.
17 Ng BG, Hackmann K, Jones MA *et al*: Mutations in the glycosylphosphatidylinositol gene PIGL cause CHIME syndrome. *Am J Hum Genet* 2012; **90**: 685–688.
18 Maydan G, Noyman I, Har-Zahav A *et al*: Multiple congenital anomalies-hypotonia-seizures syndrome is caused by a mutation in PIGN. *J Med Genet* 2011; **48**: 383–389.
19 Kvarnung M, Nilsson D, Lindstrand A *et al*: A novel intellectual disability syndrome caused by GPI anchor deficiency due to homozygous mutations in PIGT. *J Med Genet* 2013; **50**: 521–528.
20 Krawitz PM, Schweiger MR, Rodelsperger C *et al*: Identity-by-descent filtering of exome sequence data identifies PIGV mutations in hyperphosphatasia mental retardation syndrome. *Nat Genet* 2010; **42**: 827–829.
21 Krawitz PM, Murakami Y, Hecht J *et al*: Mutations in PIGO, a member of the GPI-anchor-synthesis pathway, cause hyperphosphatasia with mental retardation. *Am J Hum Genet* 2012; **91**: 146–151.
22 Krawitz PM, Murakami Y, Riess A *et al*: PGAP2 mutations, affecting the GPI-anchor-synthesis pathway, cause hyperphosphatasia with mental retardation syndrome. *Am J Hum Genet* 2013; **92**: 584–589.
23 Hansen L, Tawamie H, Murakami Y *et al*: Hypomorphic mutations in PGAP2, encoding a GPI-anchor-remodeling protein, cause autosomal-recessive intellectual disability. *Am J Hum Genet* 2013; **92**: 575–583.
24 Howard MF, Murakami Y, Pagnamenta AT *et al*: Mutations in PGAP3 impair GPI-anchor maturation, causing a subtype of hyperphosphatasia with mental retardation. *Am J Hum Genet* 2014; **94**: 278–287.
25 Chiyonobu T, Inoue N, Morimoto M, Kinoshita T, Murakami Y: Glycosylphosphatidylinositol (GPI) anchor deficiency caused by mutations in PIGW is associated with West syndrome and hyperphosphatasia with mental retardation syndrome. *J Med Genet* 2014; **51**: 203–207.
26 Martin HC, Kim GE, Pagnamenta AT *et al*: Clinical whole-genome sequencing in severe early-onset epilepsy reveals new genes and improves molecular diagnosis. *Hum Mol Genet* 2014; **23**: 3200–3211.
27 Swoboda KJ, Margraf RL, Carey JC *et al*: A novel germline PIGA mutation in Ferro-Cerebro-Cutaneous syndrome: a neurodegenerative X-linked epileptic encephalopathy with systemic iron-overload. *Am J Med Genet A* 2014; **164A**: 17–28.
28 Nakashima M, Kashii H, Murakami Y *et al*: Novel compound heterozygous PIGT mutations caused multiple congenital anomalies-hypotonia-seizures syndrome 3. *Neurogenetics* 2014; **15**: 193–200.
29 Novarino G, Fenstermaker AG, Zaki MS *et al*: Exome sequencing links corticospinal motor neuron disease to common neurodegenerative disorders. *Science* 2014; **343**: 506–511.
30 Lupski JR, Gonzaga-Jauregui C, Yang Y *et al*: Exome sequencing resolves apparent incidental findings and reveals further complexity of SH3TC2 variant alleles causing Charcot-Marie-Tooth neuropathy. *Genome Med* 2013; **5**: 57.
31 de Ligt J, Willemsen MH, van Bon BW *et al*.: Diagnostic exome sequencing in persons with severe intellectual disability. *N Engl J Med* 2012; **367**: 1921–1929.
32 Roberts WL, Myher JJ, Kuksis A, Low MG, Rosenberry TL: Lipid analysis of the glycoinositol phospholipid membrane anchor of human erythrocyte acetylcholinesterase. Palmitoylation of inositol results in resistance to phosphatidylinositol-specific phospholipase C. *J Biol Chem* 1988; **263**: 18766–18775.
33 Zoltewicz JS, Plummer NW, Lin MI, Peterson AS: oto is a homeotic locus with a role in anteroposterior development that is partially redundant with Lim1. *Development* 1999; **126**: 5085–5095.
34 Ueda Y, Yamaguchi R, Ikawa M *et al*.: PGAP1 knock-out mice show otocephaly and male infertility. *J Biol Chem* 2007; **282**: 30373–30380.
35 Zoltewicz JS, Ashique AM, Choe Y *et al*.: Wnt signaling is regulated by endoplasmic reticulum retention. *PloS One* 2009; **4**: e6191.
36 McKean DM, Niswander L: Defects in GPI biosynthesis perturb Cripto signaling during forebrain development in two new mouse models of holoprosencephaly. *Biol Open* 2012; **1**: 874–883.
37 Sparks SE, Krasnewich DM *et al*.: Congenital disorders of n-linked glycosylation pathway overview; in Pagon RA, Adam MP, Ardinger HH (eds): *GeneReviews*. Seattle, WA, USA: University of Washington. 1993.
38 Schloesser M, Hofferbert S, Bartz U, Lutze G, Lammle B, Engel W: The novel acceptor splice site mutation 11396(G->A) in the factor XII gene causes a truncated transcript in cross-reacting material negative patients. *Hum Mol Genet* 1995; **4**: 1235–1237.
39 Schloesser M, Zeerleder S, Lutze G *et al*.: Mutations in the human factor XII gene. *Blood* 1997; **90**: 3967–3977.
40 Tashima Y, Taguchi R, Murata C, Ashida H, Kinoshita T, Maeda Y: PGAP2 is essential for correct processing and stable expression of GPI-anchored proteins. *Mol Biol Cell* 2006; **17**: 1410–1420.
41 Murakami Y, Kanzawa N, Saito K *et al*.: Mechanism for release of alkaline phosphatase caused by glycosylphosphatidylinositol deficiency in patients with hyperphosphatasia mental retardation syndrome. *J Biol Chem* 2012; **287**: 6318–6325.

Supplementary Information accompanies this paper on European Journal of Human Genetics website (http://www.nature.com/ejhg)

CLINICAL REPORT

AMERICAN JOURNAL OF medical genetics PART A

A Novel *PIGN* Mutation and Prenatal Diagnosis of Inherited Glycosylphosphatidylinositol Deficiency

Taku Nakagawa,[1] Mariko Taniguchi-Ikeda,[1,2,3]* Yoshiko Murakami,[4,5] Shota Nakamura,[6] Daisuke Motooka,[6] Tomomi Emoto,[1] Wataru Satake,[3] Masahiro Nishiyama,[1] Daisaku Toyoshima,[1] Naoya Morisada,[1] Satoshi Takada,[1] Shinya Tairaku,[2,7] Nobuhiko Okamoto,[8] Ichiro Morioka,[1] Hiroki Kurahashi,[9] Tatsushi Toda,[2,3] Taroh Kinoshita,[4,5] and Kazumoto Iijima[1]**

[1]Department of Pediatrics, Kobe University Graduate School of Medicine, Kobe, Japan

[2]Division of Genetic Counseling, Kobe University Hospital, Kobe, Japan

[3]Department of Neurology/Molecular Brain Science, Kobe University Graduate School of Medicine, Kobe, Japan

[4]Department of Immunoregulation, Research Institute for Microbial Diseases, Osaka University, Suita, Osaka, Japan

[5]Laboratory of Immunoglycobiology, WPI Immunology Frontier Research Center, Osaka University, Suita, Osaka, Japan

[6]Department of Infection Metagenomics, Research Institute for Microbial Diseases, Osaka University, Suita, Osaka, Japan

[7]Department of Obstetrics and Gynecology, Kobe University Graduate School of Medicine, Kobe, Japan

[8]Department of Medical Genetics, Osaka Medical Center and Research Institute for Maternal and Child Health, Izumi, Japan

[9]Division of Molecular Genetics, Institute for Comprehensive Medical Science, Fujita Health University, Toyoake, Aichi, Japan

Manuscript Received: 16 February 2015; Manuscript Accepted: 7 September 2015

Glycosylphosphatidylinositol (GPI) anchors tether proteins to the extracellular face of eukaryotic plasma membranes. Defects in the human GPI anchor biosynthetic pathway cause inherited GPI deficiencies (IGDs) characterized by multiple congenital anomalies: dysmorphic faces, developmental delay, hypotonia, and epilepsy. We report the case of a 6-year-old boy with severe psychomotor developmental delay, epilepsy, and decreased granulocyte surface expression of GPI-anchored protein that suggested autosomal recessive GPI deficiency. The case underwent target exome sequencing to screen for IGDs. Target exome sequencing of the proband identified an apparently homozygous c.808T > C (p.Ser270Pro) mutation in *PIGN*, a gene involved in the GPI anchor biosynthetic pathway. As his parents were expecting another child, genetic carrier screening was conducted for the parents. Direct sequencing of the parents identified a

How to Cite this Article:
Nakagawa T, Taniguchi-Ikeda M, Murakami Y, Nakamura S, Motooka D, Emoto T, Satake W, Nishiyama M, Toyoshima D, Morisada N, Takada S, Tairaku S, Okamoto N, Morioka I, Kurahashi H, Toda T, Kinoshita T, Iijima K. 2015. A novel *PIGN* mutation and prenatal diagnosis of inherited glycosylphosphatidylinositol deficiency.
Am J Med Genet Part A 9999A:1–6.

Conflict of interest: none.
Parental consent: Obtained.
Ethics approval: Review Board of Osaka University and Kobe University.
Provenance and peer review: Not commissioned; externally peer reviewed.
Grant sponsor: Grant-in-Aid for Scientific Research; Grant number: C:233590363; Grant sponsor: Grants-in-Aid for Young Scientists (B); Grant number: 247910600; Grant sponsor: Ministry of Education, Culture, Sports, Science, and Technology of Japan; Grant number: 25129705.
*Correspondence to:
Mariko Taniguchi-Ikeda, M.D., Ph.D., Kobe University Graduate School of Medicine, Department of Pediatrics, 7-5-2, Kusunoki-Cho, Chuo-ku, Kobe, Kobe 650-0017, Japan. E-mail: tanimari@med.kobe-u.ac.jp
**Correspondence to:
Yoshiko Murakami, M.D., Ph.D., Osaka University, Research Institute for Microbial Diseases, Department of Immunoregulation, 3-1, Yamadaoka, Suita, Osaka 565-0871, Japan. E-mail: yoshiko@biken.osaka-u.ac.jp
Article first published online in Wiley Online Library
(wileyonlinelibrary.com): 00 Month 2015
DOI 10.1002/ajmg.a.37397

heterozygous c.808T > C *PIGN* mutation in the father but none in the mother. To identify the mother's mutation, we performed semi-quantitative real-time PCR of the *PIGN* exons and long PCR, identifying a microdeletion in *PIGN* (del exons 2–14). The proband had inherited this microdeletion from his mother. Prenatal diagnosis of the fetus revealed that it was a heterozygous carrier of the mother's pathogenic allele. Here, we report a sporadic case of inherited GPI deficiency with a *PIGN* mutation and the first case of prenatal diagnosis for GPI deficiency.

Key words: developmental defect; PIGN; prenatal diagnosis; genetic counseling; inherited GPI deficiency

INTRODUCTION

Glycosylphosphatidylinositol (GPI) anchors function as sorting signals for the transport of GPI-anchored proteins (GPI-APs) in secretory and endocytic pathways, and enable the anchoring of GPI-APs in lipid rafts of cell membranes [Kinoshita et al., 2008]. The GPI anchor biosynthetic pathway involves at least 26 gene products [Kinoshita et al., 2008], the mutations in 12 of which lead to inherited GPI deficiencies (IGDs), a subgroup of congenital disorders of glycosylation. The affected genes include *PIGA* (300868), *PIGM* (MIM 610293), *PIGV* (MIM 239300), *PIGO* (MIM 614749), *PGAP2* (MIM 614207), *PGAP3* (MIM 611801), *PIGW* (MIM 610275), *PIGQ* (MIM 605754), *PIGL* (MIM 280000), *PIGN* (MIM 614080), *PIGT* (MIM 610272), and *PGAP1* (MIM 61655) [Almeida et al., 2006; Krawitz et al., 2010, 2012; Maydan et al., 2011; Freeze et al., 2012; Johnston et al., 2012; Ng et al., 2012; Hansen et al., 2013; Kvarnung et al., 2013; Chiyonobu et al., 2014; Howard et al., 2014; Martin et al., 2014; Murakami et al., 2014].

The *PIGN*-encoded phosphatidylinositol glycan anchor biosynthesis, class N (PIGN) protein is expressed in the endoplasmic reticulum and transfers phosphoethanolamine to the first mannose of the GPI anchor [Hong et al., 2005]. Two families have thus far been reported to carry germline *PIGN* mutations causative of a GPI deficiency [Maydan et al., 2011; Ohba et al., 2014]. Fibroblasts from two affected patients showed a remarkable reduction in expression of the GPI-linked protein CD59, confirming a pathogenic influence of the mutation on GPI function [Maydan et al., 2011]. The phenotype was characterized by a gross delay in psychomotor development, seizures, dysmorphic features, and variable congenital anomalies of the heart, urinary tract, and gastrointestinal systems. The abundant expression of *PIGN* in various tissues explains the diverse phenotypic features and involvement of multiple body systems in these patients [Maydan et al., 2011], however, unlike other GPI deficiencies, hyperphosphatasia was not a feature of *PIGN* deficiency [Maydan et al., 2011; Ohba et al., 2014]. Recently, a fetus from consanguineous parents with a homozygous *PIGN* splicing mutation was reported with a congenital diaphragmatic hernia and multiple congenital anomalies. This was similar to a previously reported patient with severe GPI deficiency, carrying a *PIGA* mutation [Brady et al., 2014]. Here, we report a sporadic case of inherited GPI deficiency with a novel *PIGN* mutation and the first case of prenatal diagnosis for a GPI deficiency.

CLINCAL REPORT

The index patient was a 6-year-old boy with a severe intellectual disability, epilepsy, and mild dysmorphic features (Fig. 1A,B). He was the first child of non-consanguineous parents with no familial disease background. He was born at full term with a birth weight of 2,880 g [−0.36 standard deviation (SD)], body length of 48 cm (−0.45 SD), and head circumference of 33 cm (−0.19 SD). He was hypotonic from early infancy, and epilepsy started at the age of 3 months when he developed a fever with upper respiratory tract infections. Gradually, nystagmus became evident from 3 months of age. His skeletal anomalies were not prominent but his feet and fingers were rather small. He had met very few developmental milestones. His epileptic attacks increased in frequency with age, and were refractory to many anti-epileptic drugs such as valproate, zonisamide, clonazepam, levetiracetam, and lamotrigine. Apnea attacks were seen frequently. Brain magnetic resonance imaging (MRI) at 7 months was normal, but atrophy of the cerebellum became gradually evident around 4 years of age (Fig. 1C).

At age 6, his height was 107 cm (−2.7 SD), weight was 14.8 kg (−2.1 SD), and head circumference was 49 cm (−2.0 SD). He showed generalized muscle weakness and nystagmus with no ocular pursuit. He uttered no meaningful words. Laboratory examinations including blood cell count, renal and liver function, total bilirubin, uric acid, albumin, lactate, pyruvate, ammonia, amino acids, blood gasses, and thyroid function were all normal. Serum alkaline phosphatase levels were normal for his age. Screening for inborn errors of metabolism detected by acyl carnitine profile analysis was normal.

CYTOGENETIC RESULTS

G-banding chromosomal analysis revealed a normal karyotype (46, XY). No chromosomal deletions or duplications were detected by CGH array (data not shown). FACS analysis of granulocytes was performed to screen for IGDs as the patient possessed the characteristic features of the disease. As expected, granulocyte expression of GPI-APs such as CD16 and CD24 was reduced (Fig. 1D). Target exome sequencing of the 26 genes related to GPI-APs allowed us to identify a c.808T > C mutation in *PIGN* exon 9 that appeared to be homozygous. Although the c.808T > C mutation has previously been reported in Japan [Ohba et al., 2014], this point mutation was not found in 451 Japanese in-house control samples.

The proband had a healthy younger sister. His parents consulted our genetic counseling unit to request prenatal genetic testing for their next child at 12 weeks of gestation. Because the genetic analysis of *PIGN* was restricted to the proband at that point, we offered to carry out genetic carrier screening of the parents for IGDs. We detected a heterozygous c.808T > C mutation in *PIGN* exon 9 in the father but none in the mother. Because all of the SNPs around exon 9 were homozygous in the proband (data not shown), we suspected that an intragenic deletion had occurred. Quantitative real-time PCR analysis of *PIGN* exon 9 and long range PCR of cDNA identified a large deletion in *PIGN* (del exons 2–14) in the mother (Fig. 2A).

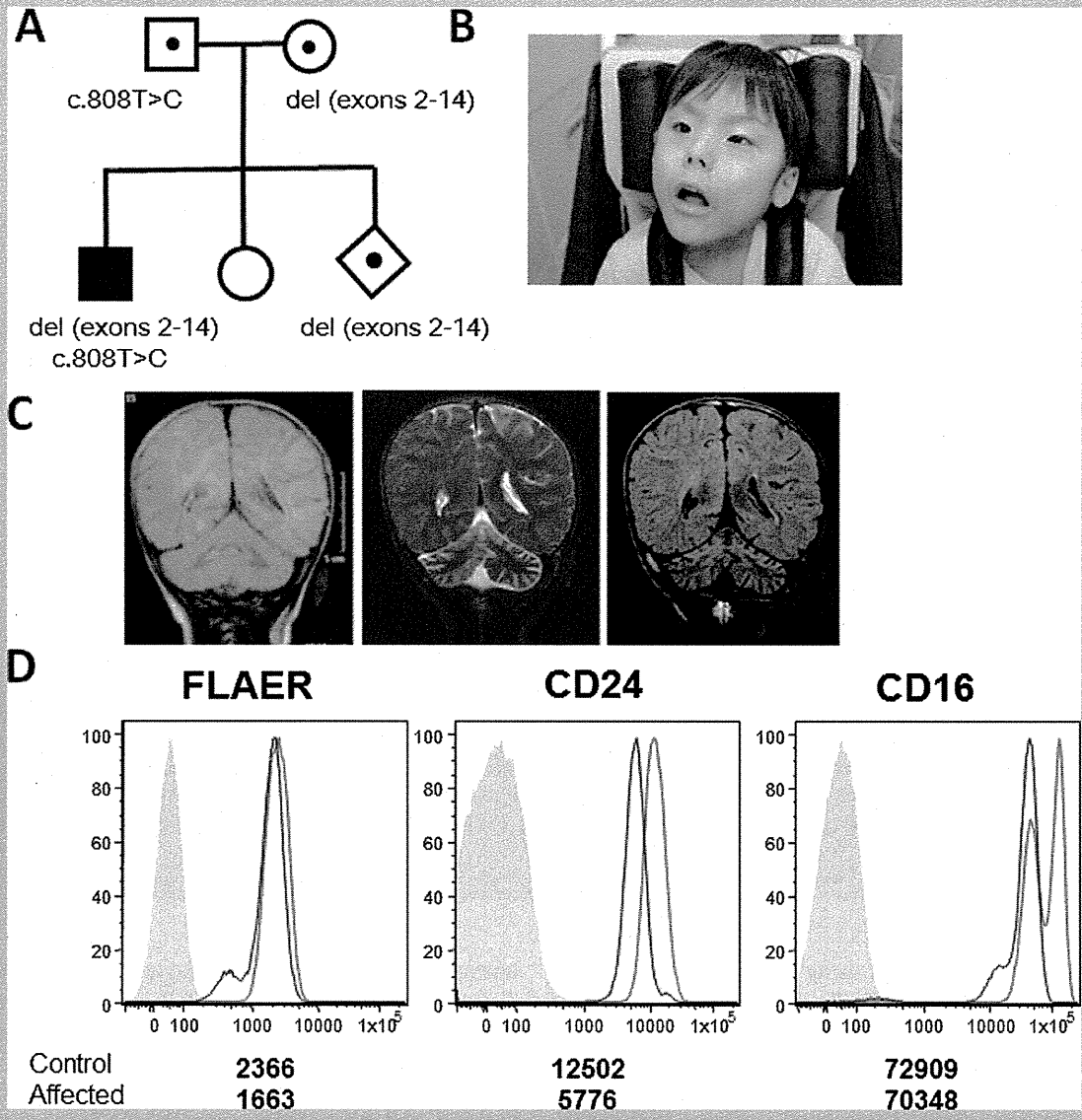

FIG. 1. Clinical features and FACS analysis of the proband's granulocytes. (A) Familial pedigree. Squares, males; circles, females; open shape, unaffected, non-carrier; black dot within shape, carrier; filled shape; IGD patient. (B) Photograph of the proband showing frontal bossing, hypertelorism, bilateral low-set ears, high nasal bridge, anteverted nares, and downturned open mouth. (C) MRI coronal imaging of the proband at: 7 months (left; FLAIR), 3 years 9 months (middle; T2-weighted image), and 5 years 9 months (right; FLAIR). Progressive atrophy of the cerebellum is noted in the middle and right image. (D) FACS analysis of granulocytes showing the surface expression of GPI-anchored proteins. Proband (blue line), normal control (red line), and an isotype control (gray shadow) are shown. CD24 expression was decreased to 46% of normal levels in the proband. Numbers indicate mean fluorescent intensities.

The deletion breakpoint was detected within introns 1 and 14 with the addition of TA at the junction (Fig. 2B). No substantial homology was found between the breakpoint regions. The proband had inherited this microdeletion from his mother (Fig. 2C). After genetic counseling, prenatal diagnosis of the fetus was performed at 16 weeks of gestation. The fetus was found to be a heterozygous carrier of the maternal pathogenic allele but lacked a paternal mutation (Fig. 2C, D), and the parents continued the pregnancy.

MATERIALS AND METHODS

Genomic Analysis of the Affected Family

We conducted genomic analysis of the proband and his parents using DNA extracted from peripheral blood samples. For prenatal diagnosis, 30 ml of amniotic fluid was collected from the fetus at 16 weeks of gestation. DNA was directly extracted using phenol-chloroform from 15 ml of amniotic fluid and the remain-

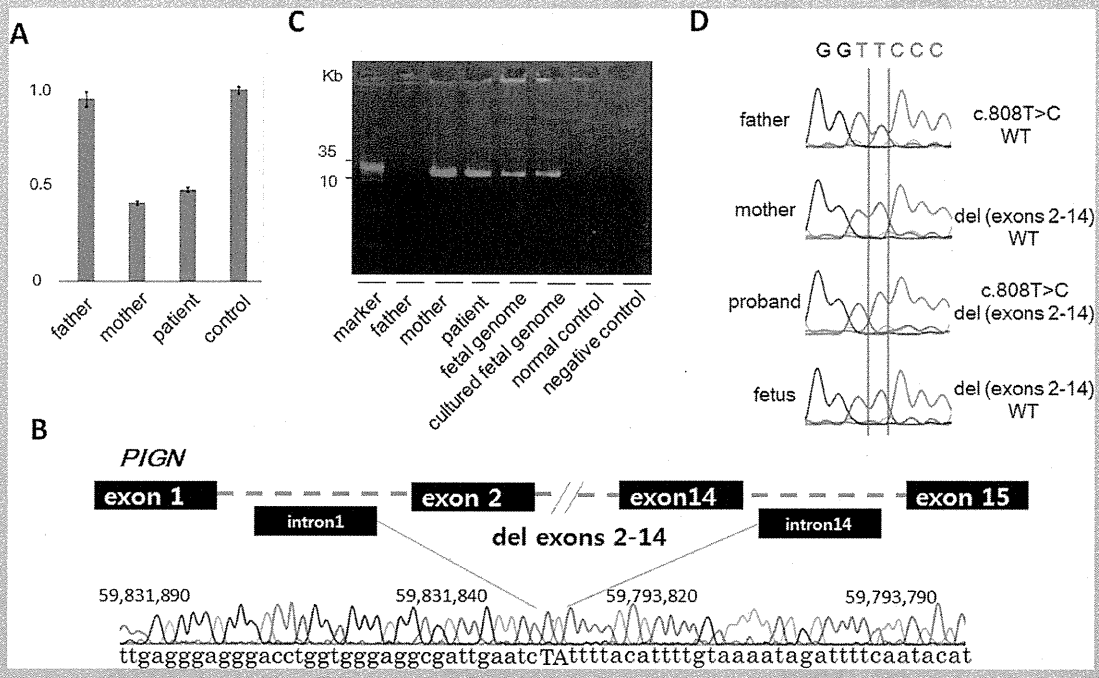

FIG. 2. Mutation analysis of the family and prenatal genetic analysis of the fetus. (A) Quantitative real time PCR analysis of *PIGN* exon 9 in the family. The control genome was normalized to 1. (B) Sequence chromatogram and schematic representation of *PIGN* microdeletion. The breakpoint is highlighted by capital letters in the sequence. (C) PCR detection of the microdeletion. A single 20-kb band, corresponding to the mutant allele, is seen in the mother, proband, and fetal genome but not in the father or normal control. Marker, molecular weight marker (Takara 2.5-kb ladder). (D) Prenatal genetic analysis of the whole family. The fetus inherited a wild-type allele from the father and a microdeletion from the mother.

der was incubated and cultured using Amniomax-II Complete Medium (Life Technologies, CA). To exclude contamination of the maternal genome, six microsatellite markers (D9S306, D9S2105, D9S2170, D9S2171, D9S2107, and D9S172) were analyzed as reported previously [Kondo-Iida et al., 1999]. Informed consent was obtained from the proband's parents, and experimental protocols and ethics approval for this study was obtained from the Review Boards of Osaka University and Kobe University. Comparative genomic hybridization (CGH) and single nucleotide polymorphism (SNP) array (180K, SurePrintG3, Agilent Technologies, CA) were performed and scanned for the proband using an Agilent DNA Microarray Scanner BA (Agilent Technologies, CA).

Target exome sequencing was performed to detect mutations in 26 genes involved in biosynthesis or remodeling of GPI-APs using the HaloPlex Exome kit (Agilent Technologies, CA) and MiSeq Sequencer (Illumina, CA). Mutations were validated by Sanger sequencing. Sequencing primers to detect point mutations were *PIGN*_exon9_F, 5′-ttactcagcaggcagtctgg-3′, and *PIGN*_exon9_R, 5′- tggcacaaatgtcaaaatga-3′. Real-time quantitative PCR was performed to detect microdeletions using standard protocols on an Applied Biosystems 7900HT real-time PCR system with the *PIGN* exon 9 primers described above. Microdeletions were also detected by long range genomic PCR using the following primers: *PIGN*_intron_1F 5′-ttgtctgataccaaaaccacagaaa-3′, and *PIGN*_intron_14R 5′-ctgaatggatggtaagaacatttcc-3′, followed by direct sequencing. Three DNA samples without microdeletions were used as control genomes. Each sample was tested in triplicate.

Total RNA was extracted from the peripheral blood of the proband and his parents using the PAXgene Blood RNA Kit (Qiagen, Venlo, Netherlands), and cDNA was synthesized with reverse transcriptase (Life Technologies, CA) using standard protocols. To detect exonic deletions, long range RT-PCR was performed using the primers *PIGN*_long_cDNAexon1f 5′-gtagtggtggcttaggaatacc-3′ and *PIGN*_long_cDNAexon19r 5′-cggtaagcatatagcggtagaaa-3′. PrimeSTAR GXL DNA Polymerase (Takara Bio, Shiga, Japan) was used for the amplification of long PCR products using standard protocols. Deleted exons were confirmed by direct sequencing.

Fluorescence Activated Cell Sorting (FACS) Analysis

FACS analysis of peripheral blood granulocytes was performed using anti-CD16 and anti-CD24 antibodies (3G8 and ML5, respectively) and GPI-binding aerolysin (FLAER) as reported previously [Chiyonobu et al., 2014].

DISCUSSION

GPI-anchored proteins are produced by most eukaryotic cells, ranging in complexity from protozoa through to vertebrates. They perform a diverse set of functions including roles in signal transduction, cell adhesion, and antigen presentation [Paulick et al., 2008]. Their importance is evidenced by the embryonic lethality of GPI-deficient mice [Nozaki et al., 1999]. Recently, several causative mutations for GPI anchor deficiency have been identified by exome sequencing. The clinical manifestation of our index patient, in particular, progressive cerebellar atrophy and nystagmus starting at early infancy, were similar to the symptoms described in patients with GPI anchor deficiency in earlier studies [Maydan et al., 2011; Ohba et al., 2014].

Prenatal diagnosis of *PIGN* deficiency by ultrasound is extremely difficult because there are no noteworthy clinical symptoms before birth [Maydan et al., 2011; Ohba et al., 2014]. Mutations in 12 genes have already been shown to be causative of IGDs, and prenatal genetic consultations for the disease are likely to increase in the future because of the high recurrent risk of 25% and the severe psychomotor disabilities experienced by affected patients. The patient in the present study harbored the c.808T > C mutation, which alters an evolutionarily conserved amino acid residue (Ser270) [Ohba et al., 2014], as well as a microdeletion in *PIGN* (del exons 2–14), which is thought to impair the production of functional protein. We predict that homozygosity of the large deletion seen in the present study would be lethal. The c.808T > C mutation has previously been reported in Japan [Ohba et al., 2014]. This c.808T > C point mutation was not found in 451 Japanese in-house control samples, but frequency of the C allele was 0.002 in the Human Genetic Variation Database of Japanese SNP database (http://www.genome.med .kyoto-u.ac. jp/SnpDB/). Although the fathers of two families reported in Japan might have originated from the same ancestor, we still could speculate that this mutation might be a founder's mutation in Japan.

Recently, Kuki et al. [2013] reported that vitamin B6 (pyridoxine) is an effective treatment of drug-resistant epileptic seizures in GPI deficiency patients. Neuronal pyridoxal phosphate deficiency caused by decreased alkaline phosphatase at the cell surface is thought to be the basis of IGD seizures, and could be ameliorated by alkaline phosphatase-independent incorporation of pyridoxine into neurons [Kuki et al., 2013]. Moreover, because vitamin B6 is widely accepted as an antiemetic agent for pregnant women, prenatal treatment for IGDs by vitamin B6 is worthy of further consideration. Although vitamin B6 is not a radical treatment, prenatal diagnosis could ameliorate symptoms of IGDs.

Breakpoints of the *PIGN* deletion in this study were located within introns 1 and 14, and an additional TA was found at the point where the two original sequences were joined to form a hybrid. No substantial homology was found between the breakpoint regions. Genomic rearrangements can be caused by replication fork stalling and template switching, or DNA double-strand breaks followed by repair by either homologous recombination or non-homologous end joining (NHEJ). Typically, the replication-based pathway is associated with regions of microhomology at the breakpoint junction, while the insertion of nucleotides of unknown origin has been observed at the junction produced by NHEJ [Kidd et al., 2010]. Based on these features, we predict that the observed deletion in the maternal allele of *PIGN* was caused by a DNA double-strand break and repair through the NHEJ pathway.

In conclusion, we present a sporadic case of *PIGN* deficiency and report for the first time the prenatal genetic testing for IGDS. With the recent identification of many causative mutations for IGDs by exome sequencing, additional, as yet undiagnosed, patients are likely to be detected in the near future. Identification and characterization of additional mutations will facilitate a comprehensive understanding of, and provide a basis for the development of, therapies for the management of IGDs.

ACKNOWLEDGMENTS

We are grateful to the proband's family for their cooperation in this study. We thank Kana Miyanagi from Osaka University for technical assistance, and Kazuhiro Kobayashi for valuable suggestions. This work was supported by a Grant-in-Aid for Scientific Research (C:233590363, YM); Grants-in-Aid for Young Scientists (B) (247910600, T.N) from the Japan Society for the Promotion of Science; the Takeda Science Foundation; a Grant-in Aid for Scientific Research on Innovative Areas (Exploring molecular basis for brain diseases based on personal genomics) from the Ministry of Education, Culture, Sports, Science, and Technology of Japan (25129705, YM); and a Health Labour Sciences Research Grant for Research on Measures for Intractable Diseases (YM).

AUTHORS' CONTRIBUTIONS

TN: patient care, and writing of the manuscript; MTI and ST: care of the family for genetic counseling and prenatal diagnosis, performing experiments, and writing of the manuscript; TE: performing experiments, and writing of the manuscript; MN, DT, NM, ST, NO: patient care, and writing of the manuscript; YM, TK, SN, DM: attending planning of patient screening system, performing experiments, data analysis, and writing of the manuscript. WS: in-house data analysis, and writing of the manuscript; IM, HK, TT, KI: attending project planning, and writing of the manuscript.

REFERENCES

Almeida AM, Murakami Y, Layton DM, Hillmen P, Sellick GS, Maeda Y, Richards S, Patterson S, Kotsianidis I, Mollica L, Crawford DH, Baker A, Ferguson M, Roberts I, Houlston R, Kinoshita T, Karadimitris A. 2006. Hypomorphic promoter mutation in PIGM causes inherited glycosylphosphatidylinositol deficiency. Nat Med 12:846–851.

Brady PD, Moerman P, De Catte L, Deprest J, Devriendt K, Vermeesch JR. 2014. Exome sequencing identifies a recessive *PIGN* splice site mutation as a cause of syndromic congenital diaphragmatic hernia. Eur J Med Genet 57:487–493.

Chiyonobu T, Inoue N, Morimoto M, Kinoshita T, Murakami Y. 2014. Glycosylphosphatidylinositol (GPI) anchor deficiency caused by mutations in *PIGW* is associated with West syndrome and hyperphosphatasia with mental retardation syndrome. J Med Genet 51:203–207.

Freeze HH, Eklund EA, Ng BG, Patterson MC. 2012. Neurology of inherited glycosylation disorders. Lancet Neurol 11:453–466.

Hansen L, Tawamie H, Murakami Y, Mang Y, ur Rehman S, Buchert R, Schaffer S, Muhammad S, Bak M, Nothen MM, Bennett EP, Maeda Y, Aigner M, Reis A, Kinoshita T, Tommerup N, Baig SM, Abou Jamra R. 2013. Hypomorphic mutations in *PGAP2*, encoding a GPI-anchor-remodeling protein, cause autosomal -recessive intellectual disability. Am J Hum Genet 92:575–583.

Howard MF, Murakami Y, Pagnamenta AT, Daumer-Haas C, Fischer B, Hecht J, Keays DA, Knight SJ, Kölsch U, Krüger U, Leiz S, Maeda Y, Mitchell D, Mundlos S, Phillips JA 3rd, Robinson PN, Kini U, Taylor JC, Horn D, Kinoshita T, Krawitz PM. 2014. Mutations in *PGAP3* impair GPI-anchor maturation, causing a subtype of hyperphosphatasia with mental retardation. Am J Hum Genet 94:278–287.

Hong Y, Kang JY, Kim YU, Shin DJ, Choy HE, Maeda Y, Kinoshita T. 2005. New mutant Chinese hamster ovary cell representing an unknown gene for attachment of glycosylphosphatidylinositol to proteins. Biochem Biophys Res Commun 335:1060–1069.

Johnston JJ, Gropman AL, Sapp JC, Teer JK, Martin JM, Liu CF, Yuan X, Ye Z, Cheng L, Brodsky RA, Biesecker LG. 2012. The phenotype of a germline mutation in *PIGA*: The gene somatically mutated in paroxysmal nocturnal hemoglobinuria. Am J Hum Genet 90:295–300.

Kidd JM, Graves T, Newman TL, Fulton R, Hayden HS, Malig M, Kallicki J, Kaul R, Wilson RK, Eichler EE. 2010. A human genome structural variation sequencing resource reveals insights into mutational mechanisms. Cell 143:837–847.

Kinoshita T, Fujita M, Maeda Y. Biosynthesis, remodelling, and functions of mammalian GPI-anchored proteins: Recent progress. J Biochem 2008;144:287–294.

Kondo-Iida E, Kobayashi K, Watanabe M, Sasaki J, Kumagai T, Koide H, Saito K, Osawa M, Nakamura Y, Toda T. 1999. Novel mutations and genotype-phenotype relationships in 107 families with Fukuyama-type congenital muscular dystrophy (FCMD). Hum Mol Genet 8:2303–2309.

Krawitz PM, Schweiger MR, Rodelsperger C, Marcelis C, Kolsch U, Meisel C, Stephani F, Kinoshita T, Murakami Y, Bauer S, Isau M, Fischer A, Dahl A, Kerick M, Hecht J, Köhler S, Jäger M, Grünhagen J, de Condor BJ, Doelken S, Brunner HG, Meinecke P, Passarge E, Thompson MD, Cole DE, Horn D, Roscioli T, Mundlos S, Robinson PN. 2010. Identity-by-descent filtering of exome sequence data identifies PIGV mutations in hyperphosphatasia mental retardation syndrome. Nat Genet 42:827–829.

Krawitz PM, Murakami Y, Hecht J, Kruger U, Holder SE, Mortier GR, Delle Chiaie B, De Baere E, Thompson MD, Roscioli T, Kielbasa S, Kinoshita T, Mundlos S, Robinson PN, Horn D. 2012. Mutations in PIGO, a member of the GPI-anchor-synthesis pathway, cause hyperphosphatasia with mental retardation. Am J Hum Genet 91:146–151.

Kuki I, Takahashi Y, Okazaki S, Kawawaki H, Ehara E, Inoue N, Kinoshita T, Murakami Y. 2013. Vitamin B6-responsive epilepsy due to inherited GPI deficiency. Neurology 81:1467–1469.

Kvarnung M, Nilsson D, Lindstrand A, Korenke GC, Chiang SC, Blennow E, Bergmann M, Stödberg T, Mäkitie O, Anderlid BM, Bryceson YT, Nordenskjöld M, Nordgren A. 2013. A novel intellectual disability syndrome caused by GPI anchor deficiency due to homozygous mutations in *PIGT*. J Med Genet 50:521–528.

Martin HC, Kim GE, Pagnamenta AT, Murakami Y, Carvill GL, Meyer E, Copley RR, Rimmer A, Barcia G, Fleming MR, Kronengold J, Brown MR, Hudspith KA, Broxholme J, Kanapin A, Cazier JB, Kinoshita T, Nabbout R, WGS500 Consortium, Bentley D, McVean G, Heavin S, Zaiwalla Z, McShane T, Mefford HC, Shears D, Stewart H, Kurian MA, Scheffer IE, Blair E, Donnelly P, Kaczmarek LK, Taylor JC. 2014. Clinical whole-genome sequencing in severe early-onset epilepsy reveals new genes and improves molecular diagnosis. Hum Mol Genet 23:3200–3211.

Maydan G, Noyman I, Har-Zahav A, Neriah ZB, Pasmanik-Chor M, Yeheskel A, Albin-Kaplanski A, Maya I, Magal N, Birk E, Simon AJ, Halevy A, Rechavi G, Shohat M, Straussberg R, Basel-Vanagaite L. 2011. Multiple congenital anomalies-hypotonia-seizures syndrome is caused by a mutation in *PIGN*. J Med Genet 48:383–389.

Murakami Y, Tawamie H, Maeda Y, Büttner C, Buchert R, Radwan F, Schaffer S, Sticht H, Aigner M, Reis A, Kinoshita T, Jamra RA. 2014. Null mutation in *PGAP1* impairing Gpi-anchor maturation in patients with intellectual disability and encephalopathy. PLoS Genet 10:e1004320.

Ng BG, Hackmann K, Jones MA, Eroshkin AM, He P, Wiliams R, Bhide S, Cantagrel V, Gleeson JG, Paller AS, Schnur RE, Tinschert S, Zunich J, Hegde MR, Freeze HH. 2012. Mutations in the glycosylphosphatidylinositol gene *PIGL* cause CHIME syndrome. Am J Hum Genet 90: 685–688.

Nozaki M, Ohishi K, Yamada N, Kinoshita T, Nagy A, Takeda J. 1999. Developmental abnormalities of glycosylphosphatidylinositol-anchor-deficient embryos revealed by Cre/loxP system. Lab Invest 79: 293–299.

Ohba C, Okamoto N, Murakami Y, Suzuki Y, Tsurusaki Y, Nakashima M, Miyake N, Tanaka F, Kinoshita T, Matsumoto N, Saitsu H. 2014. *PIGN* mutations cause congenital anomalies, developmental delay, hypotonia, epilepsy, and progressive cerebellar atrophy. Neurogenetics 15:85–92.

Paulick MG, Bertozzi CR. 2008. The glycosylphosphatidylinositol anchor: A complex membrane-anchoring structure for proteins. Biochemistry 47:6991–7000.

Pathogenic Variants in *PIGG* Cause Intellectual Disability with Seizures and Hypotonia

Periklis Makrythanasis,[1,2,10] Mitsuhiro Kato,[3,4,10] Maha S. Zaki,[5] Hirotomo Saitsu,[6] Kazuyuki Nakamura,[3] Federico A. Santoni,[1,2] Satoko Miyatake,[6] Mitsuko Nakashima,[6] Mahmoud Y. Issa,[5] Michel Guipponi,[2] Audrey Letourneau,[1] Clare V. Logan,[7] Nicola Roberts,[7] David A. Parry,[7] Colin A. Johnson,[7] Naomichi Matsumoto,[6] Hanan Hamamy,[1] Eamonn Sheridan,[7] Taroh Kinoshita,[8] Stylianos E. Antonarakis,[1,2,9,*] and Yoshiko Murakami[8,*]

Glycosylphosphatidylinositol (GPI) is a glycolipid that anchors >150 various proteins to the cell surface. At least 27 genes are involved in biosynthesis and transport of GPI-anchored proteins (GPI-APs). To date, mutations in 13 of these genes are known to cause inherited GPI deficiencies (IGDs), and all are inherited as recessive traits. IGDs mainly manifest as intellectual disability, epilepsy, coarse facial features, and multiple organ anomalies. These symptoms are caused by the decreased surface expression of GPI-APs or by structural abnormalities of GPI. Here, we present five affected individuals (from two consanguineous families from Egypt and Pakistan and one non-consanguineous family from Japan) who show intellectual disability, hypotonia, and early-onset seizures. We identified pathogenic variants in *PIGG*, a gene in the GPI pathway. In the consanguineous families, homozygous variants c.928C>T (p.Gln310*) and c.2261+1G>C were found, whereas the Japanese individual was compound heterozygous for c.2005C>T (p.Arg669Cys) and a 2.4 Mb deletion involving *PIGG*. PIGG is the enzyme that modifies the second mannose with ethanolamine phosphate, which is removed soon after GPI is attached to the protein. Physiological significance of this transient modification has been unclear. Using B lymphoblasts from affected individuals of the Egyptian and Japanese families, we revealed that PIGG activity was almost completely abolished; however, the GPI-APs had normal surface levels and normal structure, indicating that the pathogenesis of PIGG deficiency is not yet fully understood. The discovery of pathogenic variants in *PIGG* expands the spectrum of IGDs and further enhances our understanding of this etiopathogenic class of intellectual disability.

Introduction

With an estimated prevalence of approximately 1%,[1] intellectual disability is one of the most common disorders of the human population. Different definitions are available, but the general consensus is that the IQ should be below 70 and symptoms should appear during the development period and affect all aspects of adaptive functioning (conceptual, social, and practical).[2,3] Intellectual disability has several etiologies, and its genetic causes, including chromosomal aneuploidies, copy-number variants (CNVs), and monogenic disorders, are estimated to account for 25%–50% of the total cases. The identification of genic variants responsible for monogenic disorders has been revolutionized since the widespread use of high-throughput sequencing.[4,5]

Glycosylphosphatidylinositol (GPI) is a glycolipid that anchors more than 150 proteins to the cell surface. GPI-anchored proteins (GPI-APs) have various important roles on the cell surface. At least 27 genes are involved in the biosynthesis and transport of GPI-APs. Among them, those that are involved in biosynthesis of GPI are called PIG (phosphatidylinositol glycan) genes, and those that are involved in the modification of GPI after attachment to proteins are called PGAP (post-GPI attachment to proteins) genes.[6]

The first reported inherited GPI deficiency (IGD) was *PIGM* (MIM: 610273) deficiency in individuals suffering from portal thrombosis and seizures without intellectual disability.[7,8] The mutation was located in the promoter, which disrupted the binding of transcriptional factor SP1 and decreased promoter acetylation, leading to decreased expression of *PIGM*. Many more IGDs have been recently found via whole-exome sequencing (WES). Most IGDs caused by the defect in PIG genes, such as *PIGA* (MIM: 311770),[9–13] *PIGQ* (MIM: 605754),[14] *PIGY* (MIM: 610662),[15] *PIGL* (MIM: 605947),[16,17] *PIGW* (MIM: 610275),[18] *PIGV* (MIM: 610274),[19,20] *PIGN* (MIM: 606097),[21–23] *PIGO* (MIM: 614730),[24–26] and *PIGT* (MIM: 610272),[27,28] are partial deficiencies given that complete loss of function of these genes causes embryonic death.[29] These IGDs show decreased amounts of various GPI-APs and can be diagnosed by flow cytometry of granulocytes.[25] The major symptoms include intellectual

[1]Department of Genetic Medicine and Development, University of Geneva, Geneva 1211, Switzerland; [2]Service of Genetic Medicine, University Hospitals of Geneva, Geneva 1211, Switzerland; [3]Department of Pediatrics, Yamagata University Faculty of Medicine, Yamagata 990-9585, Japan; [4]Department of Pediatrics, Showa University School of Medicine, Tokyo 142-8666, Japan; [5]Department of Clinical Genetics, National Research Centre, Cairo 12311, Egypt; [6]Department of Human Genetics, Yokohama City University Graduate School of Medicine, Yokohama 236-0004, Japan; [7]School of Medicine, University of Leeds, Leeds LS2 9NL, UK; [8]Department of Immunoregulation, Research Institute for Microbial Diseases, and World Premier International Immunology Frontier Research Center, Osaka University, Osaka 565-0871, Japan; [9]Institute of Genetics and Genomics of Geneva, University of Geneva, Geneva 1211, Switzerland
[10]These authors contributed equally to this work
*Correspondence: stylianos.antonarakis@unige.ch (S.E.A.), yoshiko@biken.osaka-u.ac.jp (Y.M.)
http://dx.doi.org/10.1016/j.ajhg.2016.02.007.

disability, epilepsy, and coarse facial features. Although the symptoms are very broad, other characteristic features sometimes seen include a tented upper lip, brachytelephalangy with hypoplastic nails, hearing loss, and multiple organ anomalies, such as an aganglionic megacolon and kidney or anorectal anomalies.[9–27]

In *PGAP1* (MIM: 611655) deficiency, surface levels of GPI-APs are not affected. Similarly, GPI-AP levels in *PGAP3* (MIM: 611801) deficiency are variable and sometimes not affected. Therefore, abnormalities in these deficiencies are most likely caused by the abnormal structures of proteins' membrane anchors. In these cases, the individuals with complete deficiencies are alive and show only severe intellectual disability, often with seizures and hypotonia.[30–32] Hyperphosphatasia is a useful marker for diagnosing defects in PIG genes involved in later steps of the GPI-biosynthesis pathway, such as *PIGV* and *PIGO*, because the protein part of alkaline phosphatase (ALP) is secreted from the endoplasmic reticulum (ER) without attachment to the GPI anchor. *PGAP2* (MIM: 615817) and *PGAP3* deficiencies also show hyperphosphatasia[32–34] because once ALP is anchored to the membrane by GPI, it is released from the cell surface. Thus, the symptoms vary in severity depending upon the degree of the defect and/or position in the pathway of the affected gene.

Here, we report five individuals (from three different families) who suffer from intellectual disability and hypotonia and carry loss-of-function variants in *PIGG* (phosphatidylinositol glycan anchor biosynthesis, class G). PIGG is the enzyme that attaches ethanolamine phosphate (EtNP) to the second mannose. Different from other PIG genes, *PIGG* is not essential for GPI-AP biosynthesis. GPI-APs in *PIGG*-deficient cells are present at normal levels and have normal structures because EtNP on the second mannose is removed by *PGAP5* (HGNC-approved gene symbol: *MPPE1* [MIM: 11900]) in the ER physiologically.[35] However, the discovery of individuals with *PIGG* deficiency reveals that this step is also important for neurological development.

Subjects and Methods

Clinical Reports of Affected Individuals

This study was approved by the institutional review boards of Osaka University (Japan), Yokohama City University School of Medicine (Japan), Yamagata University (Japan), University of Geneva (Switzerland), and National Research Centre (Egypt). Ethical approval for molecular genetics research studies and data use was obtained from the South Yorkshire Research Ethics Committee (reference no. 11/H1310/1; UK). Informed consent was obtained from all examined persons or their guardians.

The affected individuals belong to three different families identified in three different studies. An overview of the clinical findings, along with a comparison to the phenotype of other IGDs, can be found in Table 1, and detailed clinical descriptions can be found in the Supplemental Note. In brief, the individuals in family EG (V:1 [EG01] and V:5 [EG02], now aged 24 and 14 years, respectively) are the offspring of a consanguineous marriage between first cousins originating from Egypt. They presented with hypotonia, seizures (at 4 months of age) that were not easily controlled by drug therapy, and profound uniform developmental delay or intellectual disability. The individual in family JP (V:6 [JP01]) was born to non-consanguineous healthy Japanese parents (Figure 1). Seizures were first noted at the age of 10 months. She developed severe psychomotor developmental delay with no speech development, autistic features, and growth retardation with a poor appetite. The individuals in family PK (V:9 [PK01] and V:10 [PK02], presently 12 and 10 years old, respectively), are offspring of a mating between first cousins of Pakistani origin (Figure 1). They had severe delay in their motor development. The first individual has had a single episode of seizures, whereas the second individual has not had any epileptic episodes.

All affected individuals from the three families had either no dysmorphic features (families JP and PK) or no common features (family EG), and the common symptoms were hypotonia, severe developmental delay, and seizures. Electroencephalography (EEG) of the individuals in family EG showed that seizures were temporal and had secondary generalization, whereas EEG of the individual in family JP showed that seizure waves were in the right parietotemporal regions and propagated to the right hemisphere (Figure 2B, lower panel). Brain MRI showed a thin corpus callosum and asymmetry of the lateral ventricles in both individuals in family EG (Figure 2A), normal findings in the individual in family JP (Figure 2B, right upper panel), and cerebellar hypoplasia and mild cerebral atrophy in both individuals in family PK (Figure 2C).

Variant Identification

Egyptian Family

Variant identification was performed as previously described.[36] In brief, all family members for whom DNA was available (noted horizontal bars, Figure 1) were genotyped with the HumanOmniExpress Bead Chip (Illumina), and the genotypes were used for identifying runs of homozygosity in each individual. Simultaneously in the eldest individual, the exome was captured with SureSelect Human All Exon V3 (Agilent), and the produced libraries were sequenced in an Illumina HiSeq 2000. Variant identification was performed with publicly available algorithms and then with genotyping data, and the variants identified through exome sequencing were combined with CATCH (Consanguinity Analysis through Common Homozygosity)[37] for the creation of a final list of candidate variants. All identified variants were confirmed by Sanger sequencing, and family segregation was confirmed.

Japanese Family

Genomic DNA was captured with the SureSelect Human All Exon V5 (Agilent Technologies) and sequenced on an Illumina HiSeq 2000 with 101 bp paired-end reads. Exome-data processing, variant calling, and variant annotation were performed as described previously.[38] Copy-number analysis using WES data was performed with eXome Hidden Markov Model v.1.0 (XHMM) as previously described.[39,40] Microdeletion involving *PIGG* was validated by quantitative real-time PCR (qPCR) on a Rotor-Gene Q thermal-cycling system (QIAGEN) with DNA from the affected individual and parents. PCR was performed in a volume of 15 μl containing 10 ng of genomic DNA, 1× Rotor-Gene SYBR Green PCR Master Mix (QIAGEN), and 1.0 μM of each primer. qPCR was carried out with the relative standard-curve method with four standard samples (30, 10, 3.33, and 1.11 ng DNA). Two primer sets for exons 7 and 12 of *PIGG* and two

reference primer sets for an area on chromosomes 9 and 15 were used. Relative copy numbers of test regions were independently calculated in comparison with those of the two reference regions and were averaged. Primer information is available on request.

Pakistani Family

Target capture was performed with the Agilent SureSelect All Exon V4 Exome Enrichment Kit according to the manufacturer's standard protocols. Sequencing of 150 bp paired-end reads was performed with an Illumina MiSeq. Reads were aligned to GRCh37 with Novoalign (Novocraft Technologies) and processed with the Genome Analysis Toolkit (GATK) and Picard (see Web Resources) for realignment of short insertions and deletions (indels) and removal of duplicate reads. Depth of coverage of the consensus coding sequence (CCDS) was assessed with the GATK, which showed that >94% of CCDS bases were covered by at least five good-quality reads (minimum Phred-like base quality of 17 and minimum mapping quality of 20). Single-nucleotide variants (SNVs) and indels were called with the UnifiedGenotyper feature of the GATK.[41,42]

Generation of LCLs, PI-PLC Treatment, and Analysis by Fluorescence-Activated Cell Sorting

Lymphoblastoid cell lines (LCLs) were generated from the affected individuals' B-lymphocytes and cultured in RPMI 1640-R2405 (Sigma-Aldrich) supplemented with 10% fetal calf serum. The LCLs were transfected with an empty pMEoriP vector or pMEoriP-humanPIGG-GST. Cells were suspended in 0.8 ml of Opti-MEM and electroporated with 20 μg each of the plasmids at 260 V and 960 mF with a Gene Pulser (Bio-Rad). Permanently transfected cells were obtained by selection with 0.5 μg/ml puromycin. Those cells were treated with or without 10 units/ml of phosphatidylinositol-specific phospholipase C (PI-PLC; Molecular Probe) for 1.5 hr at 37°C. Surface expression of GPI-APs was determined by cell staining with phycoerythrin (PE)-conjugated mouse anti-human CD59 (5H8).

Functional Assay of PIGG: Determining PIGG-Dependent Generation of Mature GPI by Analyzing GPI Mannolipids

Affected individuals' LCLs were labeled with ^{14}C-mannose. A total of 10^6 cells were incubated for 1 hr in a medium containing 100 μg/ml glucose and 10 μg/ml tunicamycin (Sigma) and then incubated in the same medium containing 0.5 μCi/ml ^{14}C-mannose (American Radiolabeled Chemicals) for 1 hr. Lipids were extracted and partitioned into n-buthanol. Glycolipids were separated on Kiesel gel 60 (Merck) and detected by a BAS-1500 image analyzer (Fujifilm). H8 indicated a complete GPI anchor, and H7 indicated a GPI-anchor intermediate without EtNP at the second mannose. A fourth mannose was added to the third mannose in H7 and H8 for the generation of H7′ and H8′, respectively. Each affected individual's cell was permanently transfected with *PIGG* cDNA or an empty vector. The positive control was lipid extracts from radiolabeled PIGK-deficient K562 cells in which the complete GPI anchor (H8) had accumulated.

Western Blotting

Lipofectamine 2000 (Invitrogen) was used for transiently transfecting HEK293 cells with SRα-promoter-driven cDNA encoding wild-type or mutant PIGG tagged with hemagglutinin (HA) at the N terminus (pME HA-hPIGG). Two days later, lysates were applied to SDS-PAGE, and HA-tagged PIGG was assessed by western blotting using anti-HA antibody.

Analysis by Fluorescence-Activated Cell Sorting

Surface levels of GPI-APs were determined by cell staining with Alexa 488-conjugated inactivated aerolysin (fluorescently-labeled inactive toxin aerolysin; Protox Biotech) and the following appropriate antibodies: PE-conjugated mouse anti-decay accelerating factor (DAF; IA10), anti-CD16 (3G8), anti-CD24 (ML5), anti-CD59 (5H8), and anti-CD48 (BJ40) antibodies (Biolegend). Cells were analyzed by flow cytometry (MACSQuant Analyzer 10, Miltenyi Biotec) with Flowjo software (v.9.5.3, Tommy Digital).

Generation of *PIGG*-Knockout HEK293 Cells

PIGG-knockout cells were generated from HEK293 cells via the CRISPR/Cas9 system. The human-codon-optimized *Streptococcus pyogenes* Cas9 and chimeric guide RNA expression plasmid pX330 were obtained from Addgene. The seed sequences for the SpCas9 target sites in *PIGG* exons 1 and 2 were selected, and a pair of annealed oligonucleotides designed according to these sequences were cloned into the BbsI sites of pX330. Lipofectamine 2000 was used for transfecting HEK293 cells with two kinds of pX330 containing the target sites. The candidate *PIGG*-knockout clones were obtained by limiting dilution and further selected by PCR and direct sequencing.

Results

Exome Sequencing and Genotyping of Family EG

After exome sequencing, 42,995,036 reads were on target in that they covered 89.12% of the coding exons as defined in RefSeq at 8×. Of the 20,119 high-quality exonic variants identified, 10,187 were synonymous and 9,021 were missense. After genotyping, we verified the correct family structure and identified that the parents share 17.9% of their genomes.

These data were combined through CATCH,[37] and after analysis of the results, three variants remained for further evaluation (Table S1) in genes *PIGG* (c.928C>T [p.Gln310*] [GenBank: NM_001127178.2]), *COQ5* (MIM: 616359; c.319G>A [p.Gly107Arg] [GenBank: NM_032314.3]), and *RGS12* (MIM: 602512; c.188A>T [p.Gln63Leu] [GenBank: NM_002926.3]). All variants were confirmed by Sanger sequencing, and family segregation confirmed that the affected individuals, as well as the unaffected siblings, are heterozygous for the variants (Figure 3A). Variants in *PIGG* and *COQ5* are not present in publically available databases, whereas the variant in *RGS12* has a cumulative frequency of 4.95e−5 in the Exome Aggregation Consortium (ExAC) Browser.[43] The variant in *PIGG* is nonsense, whereas the other two are missense.

PIGG was considered the most prominent candidate because the variant identified causes a clear loss of function. A recent inquiry of the ExAC Browser verified that no homozygous loss-of-function variants have been reported and that the most common loss-of-function variant, c.1515G>A (p.Trp505*) (GenBank: NM_001127178.2), has a minor allele frequency (MAF) of 0.0012 in the European population. This translates to a frequency of less than 1 in 600,000 individuals, compatible with a rare autosomal-recessive disorder.

Table 1. An Overview of the Affected Individuals' Symptoms and a Comparison with the Different Aspects of the Already Identified IGDs

	Clinical Syndrome						
	MCAHS2	**Ohtahara Syndrome**	**HPMRS6**	**CHIME Syndrome**	**HPMRS5**	**Inherited GPI Deficiency**	**HPMRS1**
MIM no.	300868	3008350	616809	280000	616025	610293	239300
Associated gene (MIM no.)	*PIGA* (311770)	*PIGQ* (605754)	*PIGY* (610662)	*PIGL* (605947)	*PIGW* (610275)	*PIGM* (610273)	*PIGV* (610274)
GPI-biosynthesis step[a]	GPI biosynthesis (ER cytoplasmic side)				GPI biosynthesis (ER lumen side)		
	step 1	step 1	step 1	step 2	step 4	step 6	step 7
No. of families (affected individuals)	9 (13)	1 (1)	2 (4)	6 (7)	1 (1)	2 (3)	14 (20)
Mode of inheritance (locus)	X-linked (Xp22.2)	AR (16p13.3)	AR (4q22.1)	AR (17p11.2)	AR (17q12)	AR (1q23.2)	AR (1p36.11)
Clinical Features							
DD or ID	+	+	+/−	+	+	+	+
Seizures	+ (<1 year)	+ (<1 year)	+/−	+ (<1 year)	+ (<1 year)	+	+
Hypotonia	+	+	+/−	+	+	−	+
Head circumference	ND	ND	− or microcephaly	ND	ND	ND	ND
Facial dysmorphism	+/−	NA	+	+	+	−	+
Hearing impairment	+	NA	−	+	−	−	+/−
Joint contractures	+	+	+/−	ND	ND	ND	ND
Skeletal anomalies	ND	ND	short fingers and small feet, proximal limb shortening, hip dysplasia	ND	ND	ND	hypoplastic terminal phalanges
Skin anomalies	+/−	−	−	+/−	−	−	−
Congenital heart defects	+/−	−	−	+/−	−	−	+/−
Vesicoureteral reflex or anomalies in urinary tract	+/−	−	+/−	+/−	−	−	+/−
Anorectal anomalies	−	−	−	−	−	−	+/−
CNS abnormalities in MRI	+/−	+	+/−	+/−	+	−	+
Increased serum alkaline phosphatase	+/− (mild)	−	+/− (mild)	+/−	+	−	+
Decreased GPI-AP	+	NA	+	+	+	+	+

Abbreviations are as follows: +, present; −, absent; +/−, variable; AR, autosomal recessive; MCAHS, multiple congenital anomalies-hypotonia-seizures syndrome; CHIME, colobomas, congenital heart disease, ichthyosiform dermatosis, mental retardation, and ear anomalies; HPMRS, hyperphosphatasia with mental retardation syndrome; MRT42, mental retardation, autosomal recessive 42; DD, development delay; ID, intellectual disability; NA, not applicable; and ND, not determined.
[a]Based on the review by Kinoshita.[6]

MCAHS1	HPMRS2	IGD Identified in This Study			MCAHS3	MRT42	HPMRS4	HPMRS3
614080	614749	NA			615398	611655	615716	614207
PIGN (606097)	*PIGO* (614730)	*PIGG* (not assigned)			*PIGT* (610272)	*PGAP1* (611655)	*PGAP3* (611801)	*PGAP2* (615187)
					GPI transamidase component (ER)	removal of inositol-linked acyl chain (ER)	lipid remodeling in Golgi	
step 8	step 10	step 11			step 12	step 13	step 16	step 17
9 (17)	4 (6)	1 (EG01 and EG002)	1 (JP01)	1 (PK01 and PK02)	3 (7)	5 (7)	4 (6)	4 (9)
AR (18q21.33)	AR (9p13.3)	AR (4p16.3)	AR (4p16.3)	AR (4p16.3)	AR (20q13.12)	AR (2q33.1)	AR (17q12)	AR (11p15.4)
+	+/−	+	+	+	+	+	+	+
+ (<1 year)	+	+ (4 months)	+ (10 months)	+/−	+ (<1 year)	+/−	+/−	+/−
+	+	+	+	+	+	+	+	+
− or microcephaly	− or microcephaly	ND	ND	ND	− or microcephaly	− or microcephaly	− or microcephaly	ND
+	+	+	−	−	+	−	+	+/−
−	+/−	−	−	−	+/−	−	−	+/−
ND	ND	hyperlaxity	−	−	ND	ND	ND	ND
ND	hypoplastic terminal phalanges	−	−	−	osteopenia, scoliosis delayed bone age, short arms	ND	ND	ND
−	−	−	−	−	−	−	−	−
+/−	+/−	−	−	−	+/−	−	−	+/−
+/−	−	−	−	−	+/−	−	−	−
+/−	+/−	−	−	−	+/−	−	−	+/−
+/−	+/−	thin corpus callosum	−	cerebellar hypoplasia, cerebral atrophy	+	+/−	+/−	+/−
−	+	−	−	NA	− (hypophosphatasia)	−	+	+
+	+	−	−	−	+	−	+/−	+

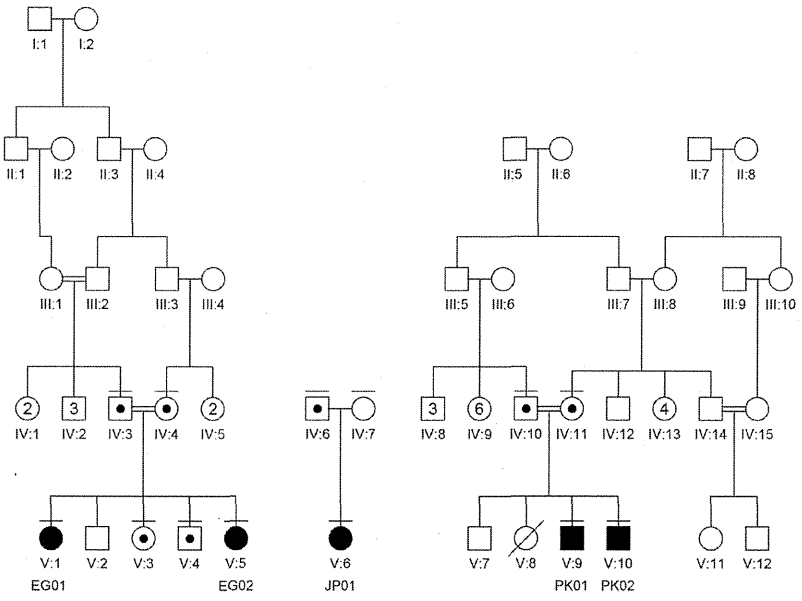

Figure 1. Family Pedigrees
The affected individuals are noted as EG01, EG02, JP01, PK01, and PK02. The family members for whom DNA was available are noted with a horizontal bar above their respective symbols. Affected individuals are homozygous or compound heterozygous for the causative variants, and family members are verified carriers. In family JP, the second variant is a de novo CNV that encompasses *PIGG*.

Exome Sequencing of Family JP

We have been conducting WES analysis of inherited intractable disorders, including infantile epilepsy, as a Japan national project since 2011. Searching WES data of 437 individuals with infantile epilepsy, we identified a *PIGG* variant (c.2005C>T [p.Arg669Cys] [GenBank: NM_001127178.2]) in the affected individual in family JP, and it seemed homozygous (no reads for the reference allele and 57 reads for the variant allele). The c.2005C>T variant was found in 4 of 575 in-house control exomes and has a MAF of 0.06% in the East Asian population according to the ExAC Browser. Web-based prediction tools suggested that the c.2005C>T variant is pathogenic (Table S1). Sanger sequencing using DNA of the affected individual and her parents revealed that the father has the heterozygous c.2005C>T variant but that the mother does not (Figure 3B). Because the affected individual showed only the variant T allele, one or two alleles with the c.2005C>T variant from her father should exist, and the maternal allele might be missing in the affected individual. In fact, a microdeletion involving *PIGG* (chr4: 60,226–2,452,836) was indicated by XHMM analysis using WES data (Figure 3C). qPCR analysis confirmed the heterozygous *PIGG* deletion in the affected individual, but not in her mother, suggesting that the microdeletion should have occurred de novo on the maternal chromosome (Figure 3D).

Exome Sequencing and Genotyping of Family PK

Custom Perl scripts were used for removing variants present in dbSNP132 or with a MAF $\geq$ 0.1% and for annotating functional consequences. We called variants in the autozygous region only with a minimum Phred-like genotype quality of 30 and selected for indels within coding regions, non-synonymous SNVs, and splice-site variants. Variants present in the 1000 Genomes dataset (November 2011), the National Heart, Lung, and Blood Institute (NHLBI) Exome Sequencing Project (ESP) Exome Variant Server, and another 2500 ethnically matched in-house exomes were also removed. This left a single variant, c.2261+1G>C (GenBank: NM_001127178.1), which was confirmed as present in the affected individuals and segregated with the phenotype in the family according to Sanger sequencing (Figure 3E).

Functional Analysis of the *PIGG* Mutants

PIGG is an EtNP transferase that mediates conversion of GPI precursor H7 to mature GPI precursor H8 (Figure S2). H8 is normally attached to proteins for the generation of GPI-APs. H7 is also competent for protein attachment, and in the absence of H8, H7 is alternatively used as an anchor. A fourth mannose can be added to H7 and H8 for the generation of H7′ and H8′, respectively. Culturing cells with radioactive mannose and analyzing the metabolically radiolabeled GPI precursors by thin-layer chromatography and phosphoimaging can be used for determining generation of H7, H7′, H8, and H8′ in cells. To determine whether *PIGG* mutations found in families EG and JP affect functional activity of PIGG, we cultured individuals' LCLs in a medium containing ^{14}C-mannose and analyzed the metabolically radiolabeled GPI precursors (Figure 4A). H7 and H7′ were accumulated in LCLs from all three affected individuals (black arrowheads [H7] and double asterisks [H7′] in lanes 4, 6, and 9 for individuals EG01, EG02, and JP01, respectively), suggesting that mutant PIGG could not add EtNP to H7 to generate H8. Such accumulation of H7 and H7′ was not seen in LCLs from a healthy individual or the father of affected individuals EG01 and EG02 (lanes 1 and 2). Importantly, these accumulation profiles of affected individuals' LCLs disappeared after transfection of normal *PIGG* cDNA (lanes 3, 5, and 8). H8 and H8′ (white arrowheads [H8] and single asterisk [H8′] in lanes 1 and 7, respectively; positive control) were not or were only weakly seen in affected individuals' LCLs, whereas they were restored by transfection of *PIGG*

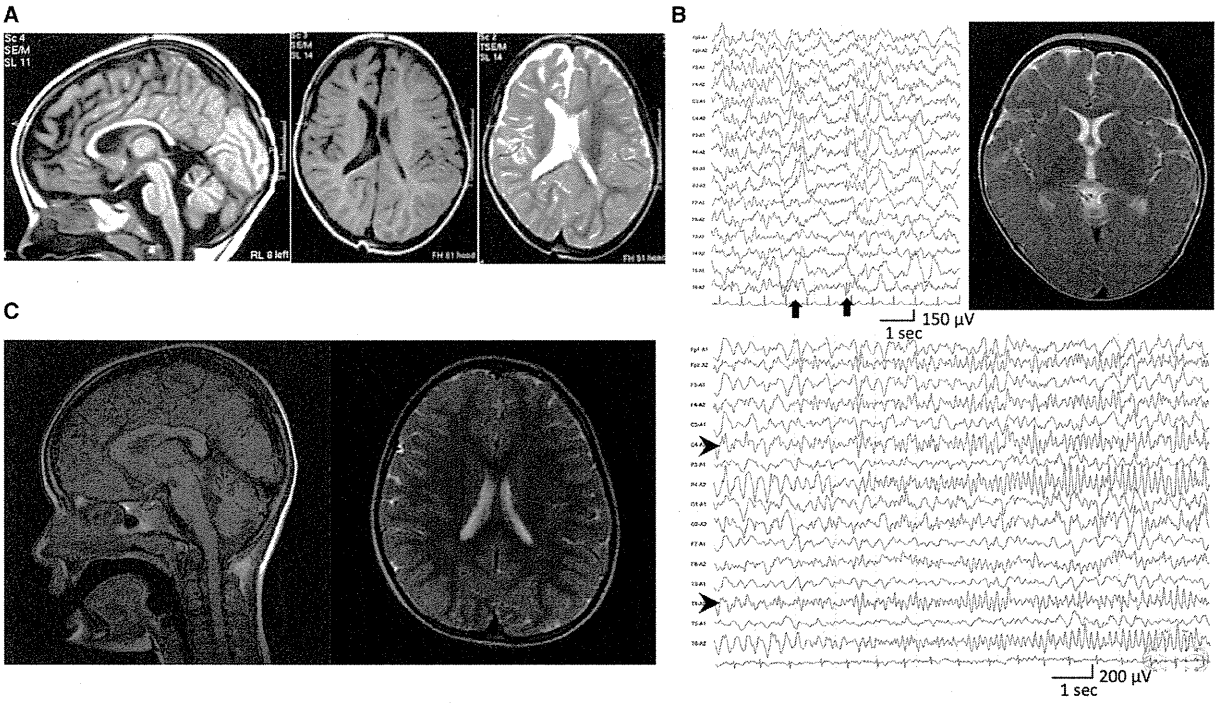

Figure 2. MRI and EEG of the Affected Individuals
(A) MRI of individual EG02 when she was 2.5 years old. (Left panel) Mid-sagittal T1-weighted MRI shows the thin corpus callosum. (Right panel) Axial plane in T1- and T2-weighted MRI shows asymmetry of the lateral ventricles.
(B) MRI and EEG of individual JP01. (Upper left panel) Interictal EEG during sleep at the age of 3 years shows focal spikes on the right posterior area (C4-P4-O2-T6, arrows). (Lower panel) Ictal EEG at 14 months shows that low-amplitude fast waves arose from right centrotemporal lesions (C4-T4, arrowheads) and then propagated to the entire right hemisphere. According to the ictal discharge, the individual developed eye deviation and head turning to the right after clonic seizures of the left upper extremity. (Upper right panel) T2-weighted brain MRI at the level of basal ganglia shows normal appearance at 11 months.
(C) MRI of individual PK01. (Left panel) Mid-sagittal T1-weighted MRI shows cerebellar hypoplasia. (Right panel) Axial plane in T2-weighted MRI shows mild cerebral atrophy.

cDNA (compare lanes 3 and 4, lanes 5 and 6, and lanes 8 and 9). These results indicate that the *PIGG* mutations in both families disrupt PIGG functional activity almost completely (Figure 4A).

It was predicted that the mutation in family EG would cause the generation of truncated PIGG because of the p.Gln310* change, whereas the p.Arg669Cys variant in family JP would not affect the apparent molecular size of PIGG. For analysis of mutant PIGG proteins, amounts of N-terminally HA-tagged wild-type, p.Gln310*, and p.Arg669Cys PIGG were detected in HEK293 cells by anti-HA antibody after western blotting. p.Gln310* PIGG was present at a high level as a truncated protein of 48 kDa, an expected size (Figure 4B). p.Arg669Cys PIGG was present at a level comparable to that of a 100 kDa wild-type PIGG, indicating that the Arg-to-Cys substitution disrupts PIGG functional activity without affecting its stability.

To investigate whether PIGG deficiency affects surface levels of GPI-APs, we used flow cytometry to analyze the granulocytes (Figure 5A) and LCLs from individuals EG01 and EG02 (Figure 5B, upper panels) and the LCLs from JP01 (Figure 4B, lower panels). Surface levels of various GPI-APs were similar on the cells of both affected individuals and healthy individuals, suggesting that they are not affected by loss-of-function mutations in *PIGG*. Making *PIGG*-knockout HEK293 cells with the CRISPR/Cas9 system further confirmed that complete loss of *PIGG* does not affect cell-surface levels of GPI-APs (Figure 5C).

Recently, individuals with *PGAP1* mutations were reported.[30] They had intellectual disability, developmental delay, encephalopathy, cerebral visual impairment, or hereditary spastic paraplegia. The complete-loss-of-function mutations in *PGAP1* did not affect the cell-surface levels of GPI-APs but caused structural abnormality of lipid moiety in GPI. Because PGAP1 removes the inositol-linked acyl chain of GPI-APs at the next step after protein attachment to the GPI anchor in the ER (Figure S2), it is possible that PGAP1 might not act on GPI-APs lacking EtNP on the second mannose in cells with mutant PIGG. Additionally, given that *PIGG* mutations caused neurological phenotypes without causing reduction in the steady-state cell-surface levels of GPI-APs (similarly to PGAP1 deficiencies), we investigated the possibility of an abnormal GPI

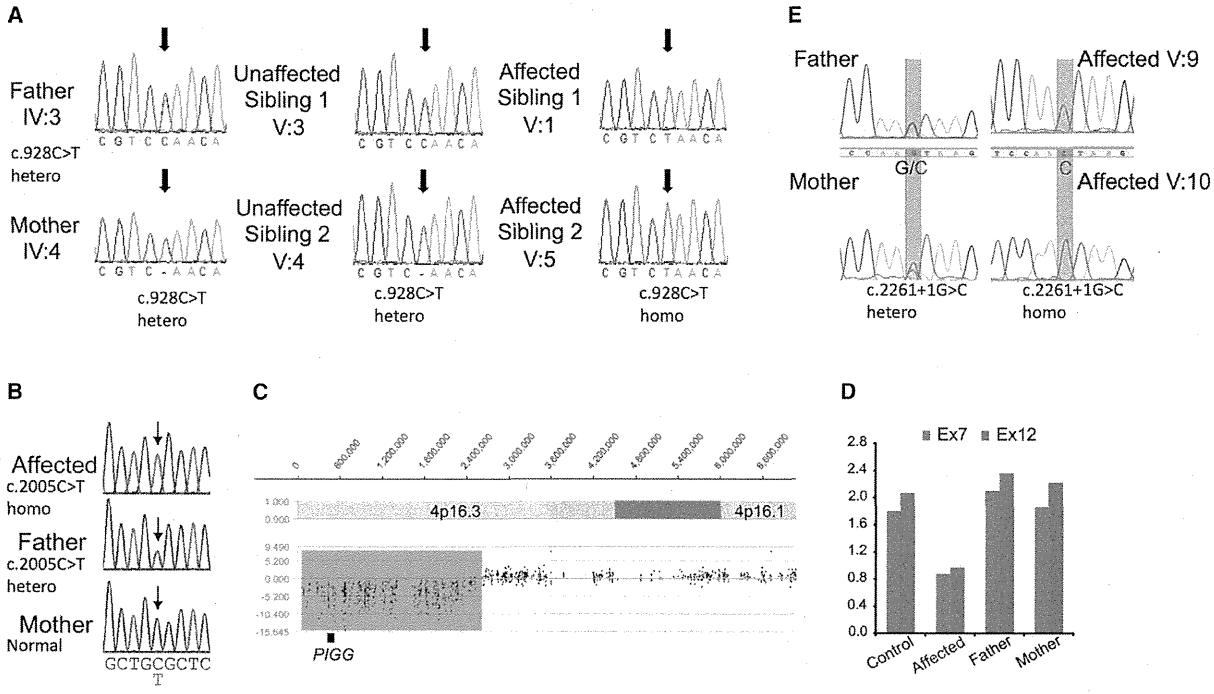

Figure 3. Identified Variants
(A) Sequencing chromatograms of the identified variant in family EG. The parents and unaffected siblings are heterozygous, whereas the affected individuals are homozygous for the c.928C>T mutation (noted by the black arrow).
(B) Sequencing chromatograms of the identified variant in family JP. The father has the heterozygous c.2005C>T variant, but the mother does not (noted by the black arrow).
(C) XHMM analysis using WES data of individual JP01. A microdeletion involving *PIGG* (chr4: 60,226–2,452,836) is indicated.
(D) qPCR analysis of exons 7 and 12 of the *PIGG* genome from individual JP01 and her parents shows a heterozygous *PIGG* deletion in the affected individual, but not in her mother, suggesting that the deletion occurred de novo on the maternal chromosome.
(E) Sequencing chromatograms of the identified variant in family PK are noted by the blue transparent boxes. The parents are heterozygous, and the affected individuals are homozygous for the c.2261+1G>C mutation.

structure. LCLs from the individuals were treated with PI-PLC, a bacterial enzyme that cleaves GPI between phosphate and glycerol and releases proteins. PI-PLC does not cleave GPI if the inositol residue is acylated. CD59 levels of *PIGG*-defective cells and *PIGG*-transfected *PIGG*-defective cells were similarly reduced by PI-PLC treatment, indicating that elimination of the acyl chain from the inositol normally occurs in LCLs from three affected individuals (Figure S1). Therefore, the structure of GPI in GPI-APs on cells with mutant *PIGG* would be normal.

Discussion

Various symptoms of IGDs are caused by reduced surface levels of GPI-APs or by abnormal GPI-AP structure. Here, we report *PIGG* deficiency, one IGD in which cells express normal surface levels of GPI-APs with a normal structure. Nevertheless, individuals from families EG and JP suffer from intellectual disability, hypotonia, and seizures, and individuals from family PK show severe intellectual disability accompanied by ataxia. In individuals from family EG, hypotonia has been remarkable since birth and remains a characteristic symptom of the disorder. Later, it was seen as hyporeflexia and a delay in achieving walking. The affected individual in family JP showed more severe developmental delay, and she could not walk or speak. In both affected individuals from families EG and JP, seizures appeared early in life, and developmental delay was also documented early in life and evolved to uniform intellectual disability. The affected individuals described here did not present with coarse faces, dysmorphic features, or other accompanying symptoms frequently seen in IGDs. Intellectual disability with seizures and severe hypotonia appear to be common characteristics of *PIGG* deficiency.

Through in vitro testing of affected individuals' LCLs, we showed that the identified variants completely abolished the function of *PIGG*, whereas the surface level of GPI-AP was normal. We obtained a similar result with *PIGG*-knockout HEK293 cells. Apparently H7 was used as an alternative GPI anchor. The EtNP transferred by PIGG to the second mannose is a transient side branch that is removed by phosphodiesterase PGAP5 in the second step after GPI is attached to the protein and that is not present in mature GPI-APs[35] (Figure S2). Therefore, the lack of this

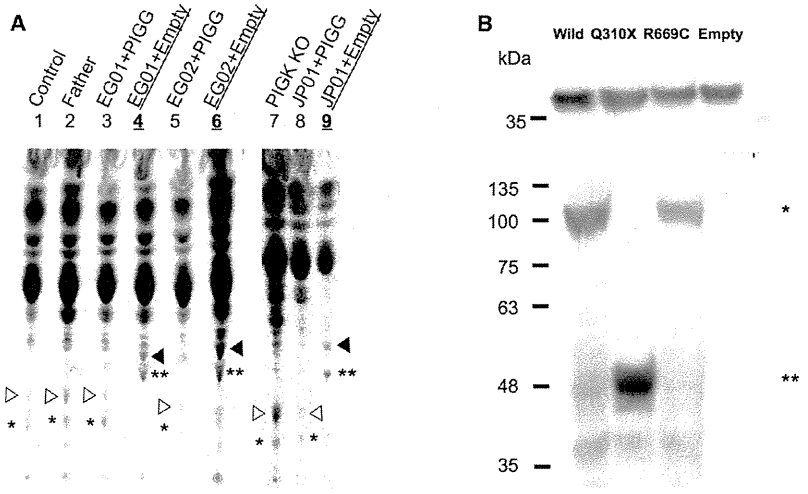

Figure 4. Functional Assays

(A) Analysis of mannolipids accumulated in LCLs from the affected individuals. Lanes are as follows: 1, LCLs from a normal individual; 2, LCLs from the father of individuals EG01 and EG02 (IV:3); 3, LCLs (transfected with *PIGG* cDNA) from individual EG01; 4, LCLs (transfected with an empty vector) from individual EG01; 5, LCLs (transfected with *PIGG* cDNA) from individual EG02; 6, LCLs (transfected with an empty vector) from individual EG02; 7, K562 PIGK-deficient cells; 8, LCLs (transfected with *PIGG* cDNA) from individual JP01; and 9, LCLs (transfected with an empty vector) from individual JP01. White arrowheads represent H8, a complete GPI intermediate, and black arrowheads represent H7, a GPI intermediate without ethanolaminephosphate at the second mannose. Asterisks indicate H7′ (*) and H8′ (**), H7 and H8, respectively, with the fourth mannose.[47]

(B) Amounts of each mutant PIGG. (Upper panel) Western blot of GAPDH for loading controls. (Lower panel) Western blot of wild-type (*) or mutant (**) HA-tagged PIGG.

transient EtNP side branch does not affect steady-state levels of cell-surface GPI-APs on B-lymphoblastoid cells and HEK293 cells (Figures 5B and 5C).

During GPI biosynthesis, EtNP is added to all three mannose residues. PIGN attaches EtNP to the first mannose at the 2-position. PIGG and PIGO attach EtNP at the 6-positions of the second and third mannoses, respectively, and share a common essential cofactor, PIGF. The EtNP attached to the third mannose, so-called "bridging" EtNP, links GPI to proteins. PIGN, PIGO, and PIGG constitute a family of EtNP transferases. In *PIGN*-defective cells, the cell-surface GPI-APs lack the EtNP side branch on the first mannose, and the surface levels are also affected. PIGN deficiency is characterized by intellectual disability, seizures, and multiple abnormalities. In *PIGO*-defective cells, the cell-surface GPI-AP levels are decreased because of a lack of or decrease in the "bridging" EtNP. PIGO deficiency causes Mabry syndrome, characterized by hyperphosphatasia, intellectual disability, seizures, and brachytelephalangy. Different from these EtNP transferase deficiencies, PIGG deficiency does not cause decreased surface expression of GPI-APs. We investigated the possibility of structural abnormality in GPI given that PGAP1 does not remove the inositol-linked acyl chain in the absence of EtNP on the second mannose and would thus cause proteins with inositol-acylated GPI to be present on the cell surface. However, this was proven not to be the case (Figure S1). In PIGG-deficient cells, therefore, GPI-APs would be normally remodeled in their fatty acid and transported to the microdomain of the plasma membrane (Figure S2). Consistent with this, PIGG-deficient individuals did not show hyperphosphatasia, which is commonly seen in PGAP3 deficiency, the fatty-acid-remodeling defect.

Another potential defect in PIGG-defective cells is that transport of GPI-APs from the ER to the cell surface is delayed. Recognition and removal of EtNP linked to the second mannose by *PGAP5* at the ER exit site is important for efficient packaging of GPI-APs into COPII-coated transport vesicles and subsequent transport to the Golgi apparatus. We investigated this possibility by using *PIGG*-knockout HEK293 cells expressing doxycycline-inducible GPI-anchored reporter protein, but we did not detect transport delay (data not shown). Although significant delay in GPI-AP transport was not detected in HEK293 cells, we still think that neuronal cells, in which many important GPI-APs need to be quickly transported to distant sites from the cell body, might require PIGG for sufficient protein attachment of GPI or for efficient GPI-AP transport from the ER to the plasma membrane. Unfortunately, the available cellular systems were not able to resolve this issue. A defect in these processes might be relevant to neurological defects seen in individuals with *PIGG* deficiency.

Although almost nothing is known about the biological function of *PIGG* in mammalian cells, important functions were reported for *GP17*, the yeast ortholog of *PIGG*. Yeast *GP17* plays an important role in cell-wall biogenesis, cell separation, and daughter cell growth.[44–46] Extensive additional experiments through the study of animal models are required for further delineating *PIGG*'s function in the human CNS.

PIGG is the 14th of the 27 known genes of the GPI-biosynthesis pathway to be associated with human disorders, suggesting that pathogenic variants in the other genes participating in GPI biosynthesis remain to be discovered in affected individuals with similar phenotypes. The complete repertoire of genes involved in

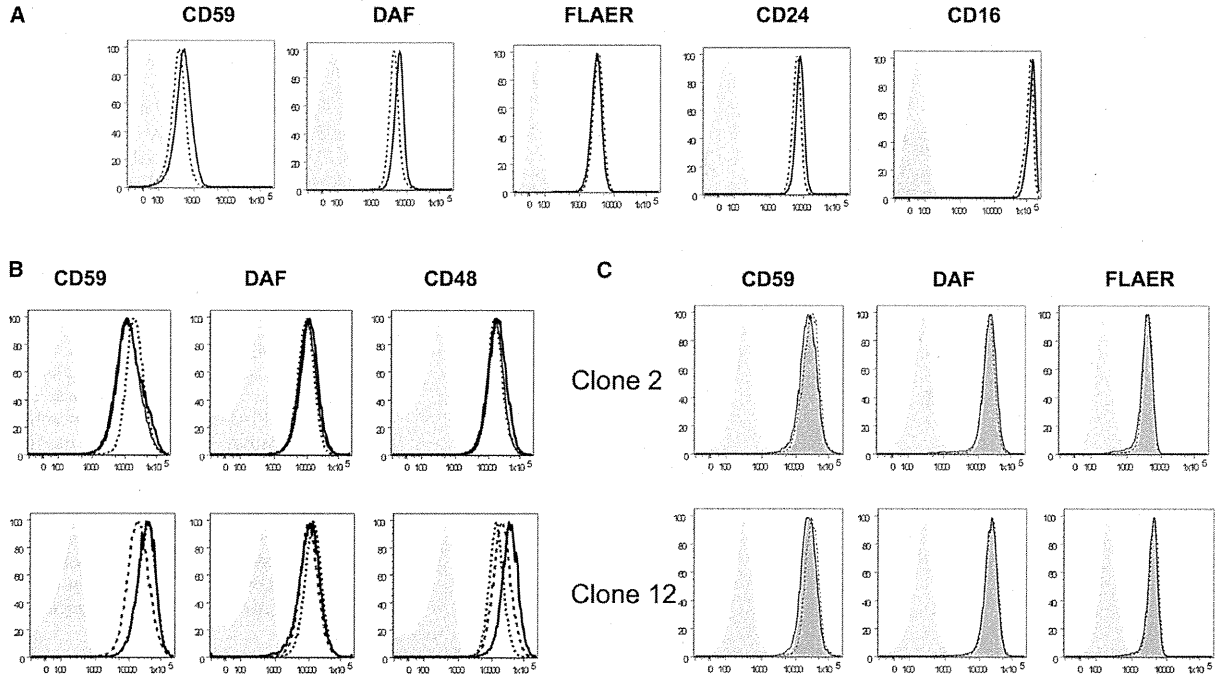

Figure 5. Flow Cytometric Analysis of Affected Individuals' Blood and Cell Lines
(A) Surface level of GPI-anchored proteins on the granulocytes from individual JP01. Thick lines represent individual JP01, dotted lines represent a healthy control individual, and gray shadows represent the isotype control.
(B) Surface level of GPI-anchored proteins on the LCLs from individuals EG01 and EG02 (upper panel) and individual JP01 (lower panel). In the upper panels, thick and thin lines represent individuals EG01 and EG02, respectively, and dotted lines represent their father. In the lower panels, thick lines represent affected individual JP01, and dotted and dashed lines represent healthy individuals. Gray shadows represent the isotype control.
(C) Surface level of GPI-anchored proteins on HEK293 cells. *PIGG*-knockout HEK293 cells were permanently transfected with *PIGG* cDNA (dotted lines) or an empty vector (thick lines). Dark-gray shadows represent wild-type HEK293 cells, and light-gray shadows represent the isotype control.

GPI-biosynthesis disorders will enhance our understanding of the pathophysiology of this form of ID and could result in treatment options for these disorders.

Supplemental Data

Supplemental Data include a Supplemental Note, two figures, and one table and can be found with this article online at http://dx.doi.org/10.1016/j.ajhg.2016.02.007.

Acknowledgments

We thank the affected individuals and their families for their participation in the study. This study was funded by grants from the Gebert Rüf Stiftung foundation to S.E.A., the von Meissner foundation to P.M., the Japan Agency for Medical Research and Development and Ministry of Health, Labour, and Welfare to Y.M., M.K., and N.M., the Japan Ministry of Education, Culture, Sports, Science, and Technology to N.M., the Japan Society of the Promotion of Science to N.M., Y.M., and H.S., and the Takeda Science Foundation to Y.M., H.S., and N.M. This work was also supported by a Sir Jules Thorn Award for Biomedical Research (JTA/09 to C.A.J. and E.S.). We also thank Dr. Abou Rami, Dr. Yusuke Maeda, and Dr. Christelle Borel for constructive discussions and Mrs. Emilie Falconnet, Pascale Ribaux, Anne Vannier, and Kana Miyanagi for their technical assistance.

Received: September 19, 2015
Accepted: February 9, 2016
Published: March 17, 2016

Web Resources

The URLs for data presented herein are as follows:

1000 Genomes, http://www.1000genomes.org/
ANNOVAR, http://www.openbioinformatics.org/annovar/
Clinical Genome Database, http://research.nhgri.nih.gov/CGD/
ClinVar, http://www.ncbi.nlm.nih.gov/clinvar/
dbSNP, http://www.ncbi.nlm.nih.gov/snp/
ELAND alignment algorithm, http://www.Illumina.com
ExAC Browser, http://exac.broadinstitute.org/
GATK, http://www.broadinstitute.org/gatk/index.php
GeneReviews, http://www.ncbi.nlm.nih.gov/books/NBK1116/
HGMD, http://www.hgmd.cf.ac.uk/ac/index.php
Human Splicing Finder, http://www.umd.be/HSF/
MutationTaster, http://www.mutationtaster.org/
NHLBI Exome Sequencing Project (ESP) Exome Variant Server, http://evs.gs.washington.edu/EVS/

NNSplice, http://www.fruitfly.org/seq_tools/splice.html
OMIM, http://www.omim.org
PolyPhen-2, http://genetics.bwh.harvard.edu/pph2/
RefSeq, http://www.ncbi.nlm.nih.gov/refseq/
SIFT, http://sift.jcvi.org/
TMHMM Server, http://www.cbs.dtu.dk/services/TMHMM/
UCSC Genome Browser, www.genome.ucsc.edu

References

1. Maulik, P.K., Mascarenhas, M.N., Mathers, C.D., Dua, T., and Saxena, S. (2011). Prevalence of intellectual disability: a meta-analysis of population-based studies. Res. Dev. Disabil. *32*, 419–436.
2. American Psychiatric Association (2013). DSM-5 Intellectual Disability Fact Sheet, http://www.dsm5.org/documents/intellectual%20disability%20fact%20sheet.pdf.
3. World Health Organization Division of Mental Health and Prevention of Substance Abuse (1996). ICD-10 Guide for Mental Retardation, http://www.who.int/mental_health/media/en/69.pdf.
4. Bamshad, M.J., Ng, S.B., Bigham, A.W., Tabor, H.K., Emond, M.J., Nickerson, D.A., and Shendure, J. (2011). Exome sequencing as a tool for Mendelian disease gene discovery. Nat. Rev. Genet. *12*, 745–755.
5. Gilissen, C., Hoischen, A., Brunner, H.G., and Veltman, J.A. (2012). Disease gene identification strategies for exome sequencing. Eur. J. Hum. Genet. *20*, 490–497.
6. Kinoshita, T. (2014). Biosynthesis and deficiencies of glycosylphosphatidylinositol. Proc. Jpn. Acad., Ser. B, Phys. Biol. Sci. *90*, 130–143.
7. Almeida, A.M., Murakami, Y., Layton, D.M., Hillmen, P., Sellick, G.S., Maeda, Y., Richards, S., Patterson, S., Kotsianidis, I., Mollica, L., et al. (2006). Hypomorphic promoter mutation in PIGM causes inherited glycosylphosphatidylinositol deficiency. Nat. Med. *12*, 846–851.
8. Almeida, A.M., Murakami, Y., Baker, A., Maeda, Y., Roberts, I.A., Kinoshita, T., Layton, D.M., and Karadimitris, A. (2007). Targeted therapy for inherited GPI deficiency. N. Engl. J. Med. *356*, 1641–1647.
9. Johnston, J.J., Gropman, A.L., Sapp, J.C., Teer, J.K., Martin, J.M., Liu, C.F., Yuan, X., Ye, Z., Cheng, L., Brodsky, R.A., and Biesecker, L.G. (2012). The phenotype of a germline mutation in PIGA: the gene somatically mutated in paroxysmal nocturnal hemoglobinuria. Am. J. Hum. Genet. *90*, 295–300.
10. Kato, M., Saitsu, H., Murakami, Y., Kikuchi, K., Watanabe, S., Iai, M., Miya, K., Matsuura, R., Takayama, R., Ohba, C., et al. (2014). PIGA mutations cause early-onset epileptic encephalopathies and distinctive features. Neurology *82*, 1587–1596.
11. Swoboda, K.J., Margraf, R.L., Carey, J.C., Zhou, H., Newcomb, T.M., Coonrod, E., Durtschi, J., Mallempati, K., Kumanovics, A., Katz, B.E., et al. (2014). A novel germline PIGA mutation in Ferro-Cerebro-Cutaneous syndrome: a neurodegenerative X-linked epileptic encephalopathy with systemic iron-overload. Am. J. Med. Genet. A. *164A*, 17–28.
12. Belet, S., Fieremans, N., Yuan, X., Van Esch, H., Verbeeck, J., Ye, Z., Cheng, L., Brodsky, B.R., Hu, H., Kalscheuer, V.M., et al. (2014). Early frameshift mutation in PIGA identified in a large XLID family without neonatal lethality. Hum. Mutat. *35*, 350–355.
13. Tarailo-Graovac, M., Sinclair, G., Stockler-Ipsiroglu, S., Van Allen, M., Rozmus, J., Shyr, C., Biancheri, R., Oh, T., Sayson, B., Lafek, M., et al. (2015). The genotypic and phenotypic spectrum of PIGA deficiency. Orphanet J. Rare Dis. *10*, 23.
14. Martin, H.C., Kim, G.E., Pagnamenta, A.T., Murakami, Y., Carvill, G.L., Meyer, E., Copley, R.R., Rimmer, A., Barcia, G., Fleming, M.R., et al.; WGS500 Consortium (2014). Clinical whole-genome sequencing in severe early-onset epilepsy reveals new genes and improves molecular diagnosis. Hum. Mol. Genet. *23*, 3200–3211.
15. Ilkovski, B., Pagnamenta, A.T., O'Grady, G.L., Kinoshita, T., Howard, M.F., Lek, M., Thomas, B., Turner, A., Christodoulou, J., Sillence, D., et al. (2015). Mutations in PIGY: expanding the phenotype of inherited glycosylphosphatidylinositol deficiencies. Hum. Mol. Genet. *24*, 6146–6159.
16. Ng, B.G., Hackmann, K., Jones, M.A., Eroshkin, A.M., He, P., Wiliams, R., Bhide, S., Cantagrel, V., Gleeson, J.G., Paller, A.S., et al. (2012). Mutations in the glycosylphosphatidylinositol gene PIGL cause CHIME syndrome. Am. J. Hum. Genet. *90*, 685–688.
17. Fujiwara, I., Murakami, Y., Niihori, T., Kanno, J., Hakoda, A., Sakamoto, O., Okamoto, N., Funayama, R., Nagashima, T., Nakayama, K., et al. (2015). Mutations in PIGL in a patient with Mabry syndrome. Am. J. Med. Genet. A. *167A*, 777–785.
18. Chiyonobu, T., Inoue, N., Morimoto, M., Kinoshita, T., and Murakami, Y. (2014). Glycosylphosphatidylinositol (GPI) anchor deficiency caused by mutations in PIGW is associated with West syndrome and hyperphosphatasia with mental retardation syndrome. J. Med. Genet. *51*, 203–207.
19. Krawitz, P.M., Schweiger, M.R., Rödelsperger, C., Marcelis, C., Kölsch, U., Meisel, C., Stephani, F., Kinoshita, T., Murakami, Y., Bauer, S., et al. (2010). Identity-by-descent filtering of exome sequence data identifies PIGV mutations in hyperphosphatasia mental retardation syndrome. Nat. Genet. *42*, 827–829.
20. Horn, D., Wieczorek, D., Metcalfe, K., Barić, I., Paležac, L., Cuk, M., Petković Ramadža, D., Krüger, U., Demuth, S., Heinritz, W., et al. (2014). Delineation of PIGV mutation spectrum and associated phenotypes in hyperphosphatasia with mental retardation syndrome. Eur. J. Hum. Genet. *22*, 762–767.
21. Maydan, G., Noyman, I., Har-Zahav, A., Neriah, Z.B., Pasmanik-Chor, M., Yeheskel, A., Albin-Kaplanski, A., Maya, I., Magal, N., Birk, E., et al. (2011). Multiple congenital anomalies-hypotonia-seizures syndrome is caused by a mutation in PIGN. J. Med. Genet. *48*, 383–389.
22. Ohba, C., Okamoto, N., Murakami, Y., Suzuki, Y., Tsurusaki, Y., Nakashima, M., Miyake, N., Tanaka, F., Kinoshita, T., Matsumoto, N., and Saitsu, H. (2014). PIGN mutations cause congenital anomalies, developmental delay, hypotonia, epilepsy, and progressive cerebellar atrophy. Neurogenetics *15*, 85–92.
23. Brady, P.D., Moerman, P., De Catte, L., Deprest, J., Devriendt, K., and Vermeesch, J.R. (2014). Exome sequencing identifies a recessive PIGN splice site mutation as a cause of syndromic congenital diaphragmatic hernia. Eur. J. Med. Genet. *57*, 487–493.
24. Krawitz, P.M., Murakami, Y., Hecht, J., Krüger, U., Holder, S.E., Mortier, G.R., Delle Chiaie, B., De Baere, E., Thompson, M.D., Roscioli, T., et al. (2012). Mutations in PIGO, a member of the GPI-anchor-synthesis pathway, cause hyperphosphatasia with mental retardation. Am. J. Hum. Genet. *91*, 146–151.
25. Kuki, I., Takahashi, Y., Okazaki, S., Kawawaki, H., Ehara, E., Inoue, N., Kinoshita, T., and Murakami, Y. (2013). Vitamin